The Astronomical Journal, 152:113 (19pp), 2016 November doi:10.3847/0004-6256/152/5/113

ROTATION IN THE PLEIADES WITH *K*2. I. DATA AND FIRST RESULTS

L. M. Rebull[1,2], J. R. Stauffer[2], J. Bouvier[3,4], A. M. Cody[5], L. A. Hillenbrand[6], D. R. Soderblom[7,8], J. Valenti[7,8], D. Barrado[9], H. Bouy[9], D. Ciardi[10], M. Pinsonneault[11,12], K. Stassun[13,14], G. Micela[15], S. Aigrain[16], F. Vrba[17], G. Somers[11,12], J. Christiansen[10], E. Gillen[16,18], and A. Collier Cameron[19]

[1] Infrared Science Archive (IRSA), Infrared Processing and Analysis Center (IPAC), 1200 E. California Blvd., California Institute of Technology, Pasadena, CA 91125, USA; rebull@ipac.caltech.edu
[2] Spitzer Science Center (SSC), Infrared Processing and Analysis Center (IPAC), 1200 E. California Blvd., California Institute of Technology, Pasadena, CA 9112, USA
[3] Université de Grenoble, Institut de Planétologie et d'Astrophysique de Grenoble (IPAG), F-38000 Grenoble, France
[4] CNRS, IPAG, F-38000 Grenoble, France
[5] NASA Ames Research Center, Kepler Science Office, Mountain View, CA 94035, USA
[6] Astronomy Department, California Institute of Technology, Pasadena, CA 91125, USA
[7] Space Telescope Science Institute, 3700 San Martin Dr., Baltimore, MD 21218, USA
[8] Center for Astrophysical Sciences, Johns Hopkins University, 3400 North Charles St., Baltimore, MD 21218, USA
[9] Centro de Astrobiología, Dpto. de Astrofísica, INTA-CSIC, E-28692, ESAC Campus, Villanueva de la Cañada, Madrid, Spain
[10] NASA Exoplanet Science Institute (NExScI), Infrared Processing and Analysis Center (IPAC), 1200 E. California Blvd., California Institute of Technology, Pasadena, CA 91125, USA
[11] Department of Astronomy, The Ohio State University, Columbus, OH 43210, USA
[12] Center for Cosmology and Astroparticle Physics, The Ohio State University, Columbus, OH 43210, USA
[13] Department of Physics and Astronomy, Vanderbilt University, Nashville, TN 37235, USA
[14] Department of Physics, Fisk University, Nashville, TN 37208, USA
[15] INAF—Osservatorio Astronomico di Palermo, Piazza del Parlamento 1, I-90134, Palermo, Italy
[16] Department of Physics, University of Oxford, Keble Rd., Oxford OX3 9UU, UK
[17] US Naval Observatory, Flagstaff Station, P.O. Box 1149, Flagstaff, AZ 86002, USA
[18] Astrophysics Group, Cavendish Laboratory, J.J. Thomson Avenue, Cambridge CB3 0HE, UK
[19] School of Physics and Astronomy, University of St. Andrews, North Haugh, St. Andrews, Fife KY16 9SS, UK
Received 2016 April 29; revised 2016 May 31; accepted 2016 May 31; published 2016 October 11

ABSTRACT

Young (125 Myr), populous (>1000 members), and relatively nearby, the Pleiades has provided an anchor for stellar angular momentum models for both younger and older stars. We used *K*2 to explore the distribution of rotation periods in the Pleiades. With more than 500 new periods for Pleiades members, we are vastly expanding the number of Pleiades with periods, particularly at the low-mass end. About 92% of the members in our sample have at least one measured spot-modulated rotation period. For the ∼8% of the members without periods, non-astrophysical effects often dominate (saturation, etc.), such that periodic signals might have been detectable, all other things being equal. We now have an unusually complete view of the rotation distribution in the Pleiades. The relationship between P and $(V-K_s)_0$ follows the overall trends found in other Pleiades studies. There is a slowly rotating sequence for $1.1 \lesssim (V-K_s)_0 \lesssim 3.7$ and a primarily rapidly rotating population for $(V-K_s)_0 \gtrsim 5.0$. There is a region in which there seems to be a disorganized relationship between P and $(V-K_s)_0$ for $3.7 \lesssim (V-K_s)_0 \lesssim 5.0$. Paper II continues the discussion, focusing on multiperiod structures, and Paper III speculates about the origin and evolution of the period distribution in the Pleiades.

Key words: globular clusters: individual (Pleiades) – stars: rotation

Supporting material: figure set, machine-readable tables

1. INTRODUCTION

The three most fundamental parameters of a star are its mass, its composition, and its angular momentum. Together, they determine how the star evolves from birth through the pre-main-sequence phase to main-sequence hydrogen burning, and beyond, and further, whether and how planets form and migrate. Angular momentum evolution is tied during star formation to cloud core fragmentation processes and stellar multiplicity, and during pre-main-sequence evolution to star–disk interactions coupled with simple radial contraction and internal structural changes. Main-sequence angular momentum evolution is dominated by spin-down due to mass loss and core-envelope coupling efficiencies. Although theoretical guidance addressing these matters for stars from Myr to Gyr ages has been significant (see, e.g., Bouvier et al. 2014 and references therein), the problems to be addressed are still lacking in empirical guidance in critical areas.

Because the Pleiades is populous (over 1000 members; e.g., Bouy et al. 2015), relatively young (125 Myr; Stauffer et al. 1998b), and nearby (136 pc; Melis et al. 2014), it has provided an anchor for stellar angular momentum models for both younger and older stars. As such, we need a thorough understanding of the rotational distribution of stars in the Pleiades. There is ample evidence that angular momentum evolution depends on stellar mass, so obtaining a reliable rotation distribution for stars of a wide range of masses is critically important. The NASA *K*2 mission (Howell et al. 2014), using the repurposed 1 m *Kepler* spacecraft, observed the Pleiades cluster nearly continuously for 72 days, enabling us to probe rotation rates to lower masses and to higher precision than ever before.

The Pleiades has been extensively studied for decades (e.g., Trumpler 1921; Hertzsprung 1947; Johnson & Mitchell 1958), and more recent surveys (e.g., Lodieu et al. 2012; Sarro

Table 1
Star Counts

Name	Number	Description
Initial sample	1020	All *K*2 LCs of candidate Pleiades members.
Best members	775	Highest-confidence (our determination) Pleiades members with *K*2 light curves, and neither too bright nor too faint ($6 < K_s < 14.5$).
OK members	51	Lower-confidence (our determination) Pleiades members with *K*2 light curves, and neither too bright nor too faint ($6 < K_s < 14.5$).
The sample, aka the sample of members	826	The set of all high-confidence ("best") plus lower-confidence ("ok") members that are neither too bright nor too faint ($6 < K_s < 14.5$), aka "members of the right brightness range."
The periodic sample	759	The subset of all high-confidence ("best") plus lower-confidence ("ok") members that are neither too bright nor too faint ($6 < K_s < 14.5$) and are found to be periodic by us in these *K*2 data.

et al. 2014; Bouy et al. 2015) have identified candidate members down to at least ~0.03 $M_\odot$ ($K_s \sim 18$, or $R > 22$), past where *K*2 can obtain a viable light curve (LC) in the Pleiades ($K_s \sim 14.5$, or $K_p \sim 18$). More than 1000 candidate members for the Pleiades were included in *K*2's Campaign 4, down to mass ~0.09 $M_\odot$.

The rotation of stars in the Pleiades has been the subject of study for quite some time, both spectroscopically (e.g., Anderson et al. 1966; Stauffer & Hartmann 1987, Soderblom et al. 1993a, 1993b; Queloz et al. 1998; Terndrup et al. 2000) and photometrically (e.g., Stauffer & Hartmann 1987; Stauffer et al. 1987; van Leeuwen et al. 1987; Prosser et al. 1993a, 1993b, 1995). There have been two recent extensive photometric surveys of Pleiades rotation periods. Hartman et al. (2010) used the Hungarian Automated Telescope Network (HATNet) to obtain rotation periods for nearly 400 Pleiades members down to $M \sim 0.4\,M_\odot$, with estimated completeness to $M \sim 0.7\,M_\odot$. More recently, Covey et al. (2016) present new rotation period observations for more than 100 Pleiads from the Palomar Transient Facility (PTF), which greatly expanded the known periods for lower-mass Pleiads down to $M \sim 0.18\,M_\odot$. These ground-based surveys, however, necessarily were biased toward larger amplitude variability, and against periods near ~1 day.

Because *K*2 provides precision, sensitivity, and continuous (as opposed to diurnal) time coverage, in the present paper we push the known periods down to lower mass and lower amplitude than has ever been done before in the Pleiades. In the process of doing this, we have found other repeated patterns in the LCs. We have already scoured the *K*2 data for eclipsing binaries (David et al. 2015, 2016). Other periods that do not appear to be spot-modulated rotation periods are included in the Appendix B. The rest of the periods are nearly all consistent with spot-modulated rotation periods (though a few are likely pulsation; see Paper II).

In Section 2, we present the observations and data reduction, as well as assembly of Pleiads members out of the 1020 *K*2 LCs of candidate Pleiads. The overall distribution of *K*2-derived rotation rates is discussed in Section 3. Section 4 summarizes our main results.

This is the first of three papers focused on rotation periods in the Pleiades. Paper II, Rebull et al. (2016), discusses the several types of LCs and periodogram structures that we found in the *K*2 data, as well as some of the properties of these multiperiod stars. Stauffer et al. (2016), Paper III, speculates about the origin and evolution of the period distribution in the Pleiades.

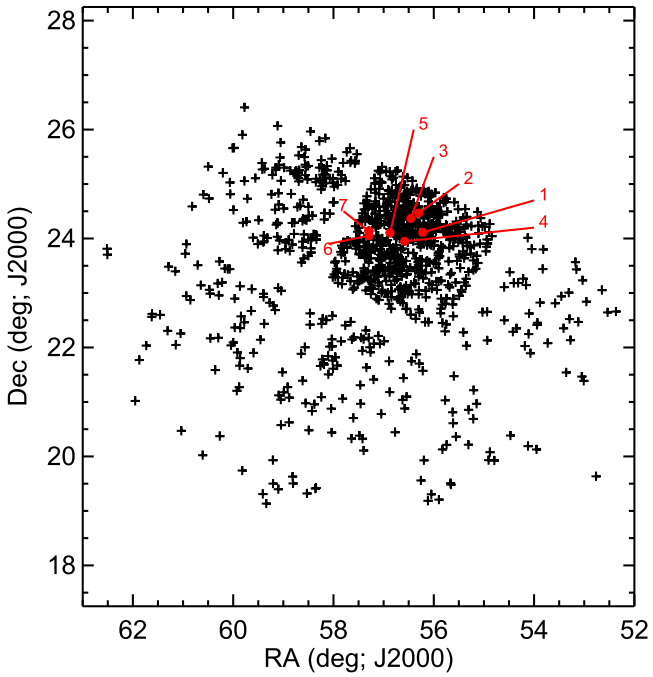

Figure 1. All 1020 candidate Pleiades members with *K*2 LCs projected onto the sky. Red numbers correspond as follows: 1-Electra = HII468; 2-Taygeta = HII563; 3-Maia = HII785; 4-Merope = HII980; 5-Alcyone = etaTau = HII1432; 6-Atlas = HII2168; 7-Pleione = HII2181. Note that the entire Pleiades cluster, centered roughly on Alcyone, is not included in the *K*2 fields; the tidal radius of the Pleiades is ~6°. Note also the gaps between *K*2 detectors.

2. OBSERVATIONS AND METHODS

2.1. K2 Data

Members of the Pleiades were observed in *K*2 Campaign 4, which lasted for 72 days. Note that the field of view is not centered on the cluster; see Figure 1. All of the stars shown were observed in the long-cadence (~30-minute exposure) mode. Thirty-four of these stars were additionally observed in fast cadence (~1-minute exposure), but those data are beyond the scope of the present paper. There are 1020 unique *K*2 long-cadence LCs (this is the number given in Table 1 as the "initial sample").

Kepler pixel sizes are relatively large, 3.″98 × 3.″98, and the 95% encircled energy diameter ranges from 3.1 to 7.5 pixels with a median value of 4.2 pixels. During the *K*2 portion of the mission, because only two reaction wheels can be used,

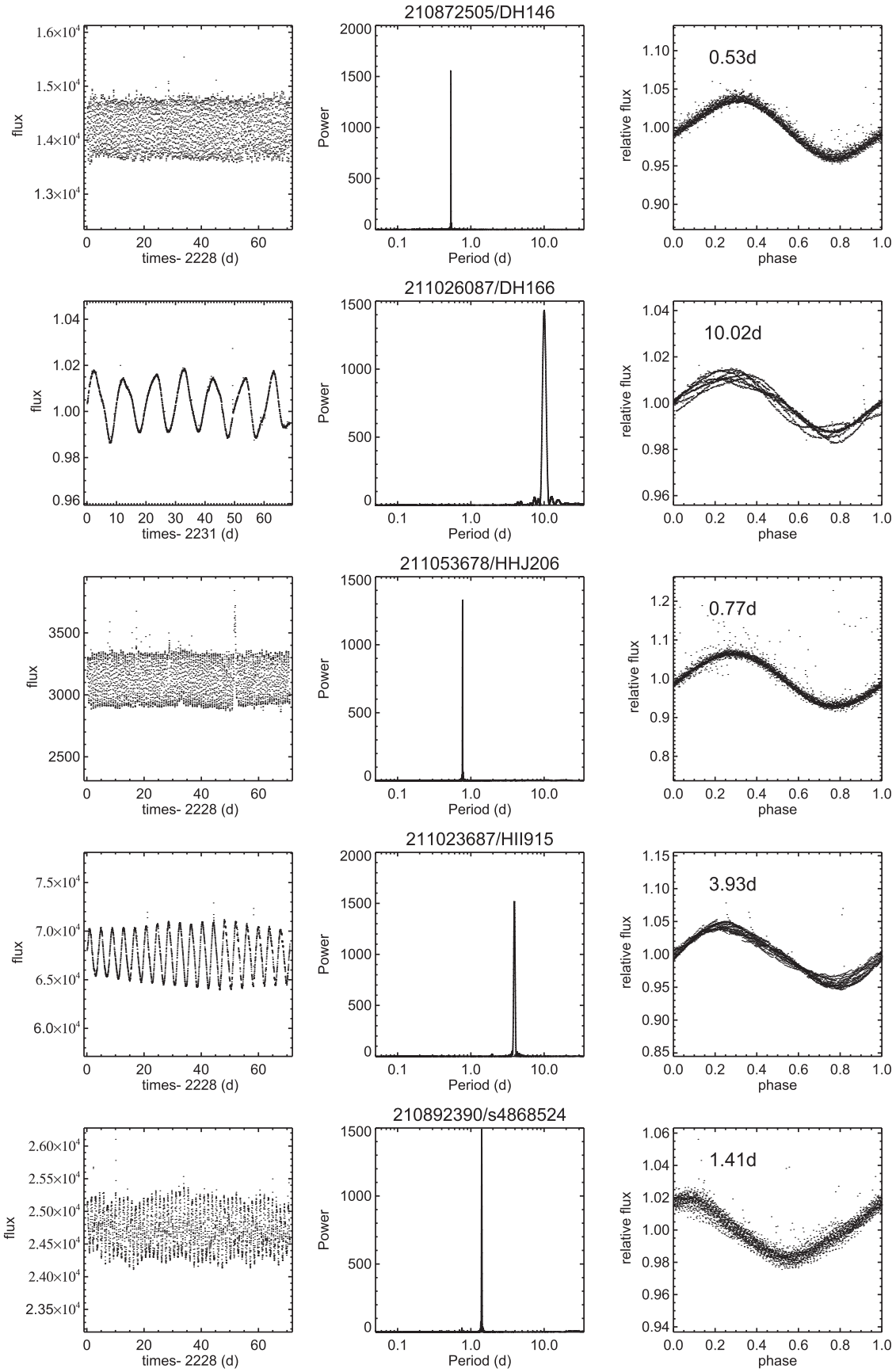

Figure 2. Five examples of finding periods in the *K*2 Pleiades data. Left column: full LC; middle column: LS periodogram; right column: phased LC, with best period (in days) as indicated. Rows, in order: EPIC 210872505/DH146, 211026087/DH166, 211053678/HHJ206, 211023687/HII915, 210892390/s4868524. These are representatives from a range of brightnesses and periods. Note that in each case, the power spectrum indicates unambiguously periodic signals—the peak is so high that little structure other than the peak can be seen in the power spectrum. These LCs are best interpreted as large spots or spot groups rotating into and out of view.

the whole spacecraft slowly drifts and then repositions regularly every 0.245 days.

We have used several different sets of LCs employing different reductions: (1) the pre-search data conditioning (PDC) version generated by the *Kepler* project and obtained from MAST, the Mikulski Archive for Space Telescopes; (2) a version with moving apertures obtained following A. M. Cody et al. (2016, in preparation); (3) a version using a semiparametric Gaussian process model used by Aigrain et al. (2015, 2016); (4) the "self-flat-fielding" approach used by Vanderburg & Johnson (2014) as obtained from MAST. We removed any data points corresponding to thruster firings and any others with bad data flags set in the corresponding data product. The times (as shown in figures in this and our subsequent papers) are *Kepler* baricentric Julian day.

We inspected LCs from each reduction approach, and we selected the visually "best" LC from among the four, such as the LC with the least discontinuities, or the one with the least overall trend, or the one least subject to saturation effects, etc. Out of our entire sample of 1020 LCs, the PDC LC was the best for ∼58% of the sample, 11% of the LCs had the best version from Aigrain et al., ∼8% had the best version from A. M. Cody et al., and ∼5% of the LCs were best in the Vanderburg & Johnson approach. It is important to note that in most cases, the period appears as a significant peak in the periodograms for all four LC versions, but the subtleties of the processing mean that one version is slightly better than another and is the one that we used to obtain the periods reported here. In general, the PDC LC was best for $\lesssim$3 days; both the Aigrain and Vanderburg approaches were on average best for the longer periods. For ∼18% of the 1020, it was not clear which was the best LC, either because the LC was saturated (too bright) or too faint, or adversely affected by nearby bright stars, or all the LC versions were different enough that no one LC could be selected as the best and most reliable. None of these latter confusing LCs were found to be periodic.

In two cases, there are pairs of light curves that are indistinguishable. EPIC 211076026 and 211076042 are ADS2755A and ADS2755B, which are sometimes jointly referred to as HII956 or HD 23479. These two stars are a visual binary with a separation of ∼0.″7, so close that the *K*2 LCs are effectively identical. We dropped 211076026 and kept 211076042; the LC is not periodic. EPIC 211066337 (HII298) and EPIC 211066412 (HII299) are functionally indistinguishable LCs. They are a visual binary separated by ∼6″. We have kept EPIC 211066337 and dropped EPIC 211066412. The net LC in EPIC 211066337 has two periods, 6.156 and 2.932 days, and we suspect that there is one period per binary component (see Paper II).

2.2. Finding Periods

We looked for periodic signals using primarily the NASA Exoplanet Archive Periodogram Service[20] (Akeson et al. 2013). This service provides period calculations using Lomb–Scargle (LS; Scargle 1982), Box-fitting Least Squares (Kovács et al. 2002), and Plavchan (Plavchan et al. 2008) algorithms. We also looked for periods using CLEAN (Roberts et al. 1987).

[20] http://exoplanetarchive.ipac.caltech.edu/cgi-bin/Periodogram/nph-simpleupload

In practice, though, the periodic signals are generally not ambigous and any method yields very similar periods. Different LC versions can make more of a difference in the derived period than different period-finding algorithms because of the influence of artifacts. We used LS for the analysis discussed here, because most of the periodic signals are sinusoidal.

Some LCs, periodograms, and phased LCs can be found in Figure 2. These are representatives from a range of brightnesses and periods. The power spectra indicate unambiguously periodic signals—the peak is so high that little structure other than the peak can be seen in the power spectrum, and when there is substructure, it is a harmonic of the main signal. (However, see Paper II for multiperiodic stars.) For signals like those in Figure 2, the false-alarm probability (FAP) returned by the LS algorithm is 0; for ∼97% of the sample with periods, the FAP of the main peak is very small, ∼0. For many stars, the FAP of the second or third peak is *also* ∼0, which gives rise to the multiperiodic discoveries in Paper II. The only situations in which we took a star to be periodic when the FAP for the peak calculated over the whole LC was not ∼0 were situations in which, e.g., half the LC was corrupted by instrumental effects and thus we took a P derived from the unaffected portion (which then meant that the FAP computed for that peak on that portion of the LC was very low), or the three stars in Section 2.3.1 where there is a clear peak at the same location as others found for this star in an independent data set, even if the formal FAP calculated for that peak from the *K*2 data was high.

For stars of the mass range considered here, the periods that we measure are, by and large, star spot-modulated rotation periods. Spot modulation is the simplest explanation for sinusoidal (or sinusoidal-like) variations where there are changes over an entire rotation phase.

To be conservative, we required at least 2 complete cycles of a pattern to call it periodic; thus, the maximum period we searched for was 35 days. We do not expect Pleiades members to be rotating more slowly than 35 days. Indeed, the distribution of periods we found (see Figure 3) is strongly peaked at $<$1 day; only ∼3% of the periods over all 1020 LCs (not just members identified in Section 2.5 below) are longer than 10 days. Because the number of rotation periods falls off so strongly, we suspect that few or no legitimate rotation periods of Pleiades members are $>$35 days, and our approach is not unduly biasing our derived distribution of rotation periods in the Pleiades. There may be some patterns that are repeated on timescales longer than 35 days, but they are not rotation periods—the shapes of the LCs are much different than the rotation periods in the data.

Additionally, by inspection of individual LCs, we deemed some periodic signals with periods shorter than 35 days to not necessarily be rotation periods. Two objects, EPIC 211082420 (HII1431) and EPIC 210822691 (AKII465), are eclipsing binaries (see David et al. 2015, 2016). We have removed these periods from our sample because they are not spot-modulated rotation periods (AKII465 is also likely not a member of the Pleiades). There are other eclipsing binaries in our data, but for those, there is also a periodic signal from the primary, which we retain here because it is likely to be a rotation rate; see, for example, EPIC 211093684/HII2407 in David et al. (2015). There are 28 additional objects that have features in their LS periodograms that suggest possible periods $P < 35$ days, but that which we believe are not unambiguously

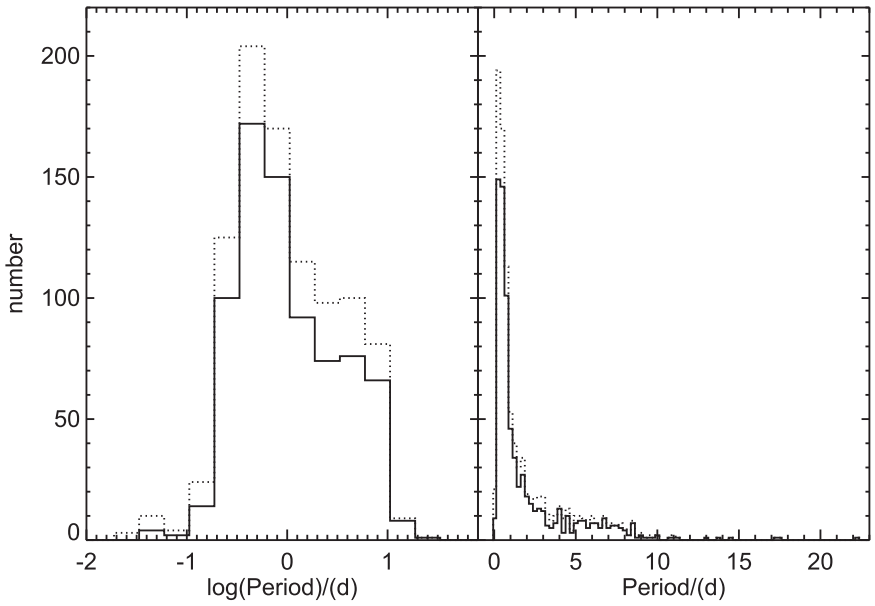

Figure 3. Histograms, on the left of the log of periods, and on the right of the linear periods, found by our analysis, in days. Solid line is the primary period (that which we take to be the rotation period of the star), and dotted line is (for reference) a histogram of all the periods found here, including the secondary, tertiary, and quaternary periods (see Paper II). We limited our search to $P < 35$ days, half our campaign length, but strongly suspect that no legitimate rotation periods of Pleiades members are >35 days (1.54 in the log). The period distribution is strongly peaked at <1 day, with the maximum P at 22.14 days.

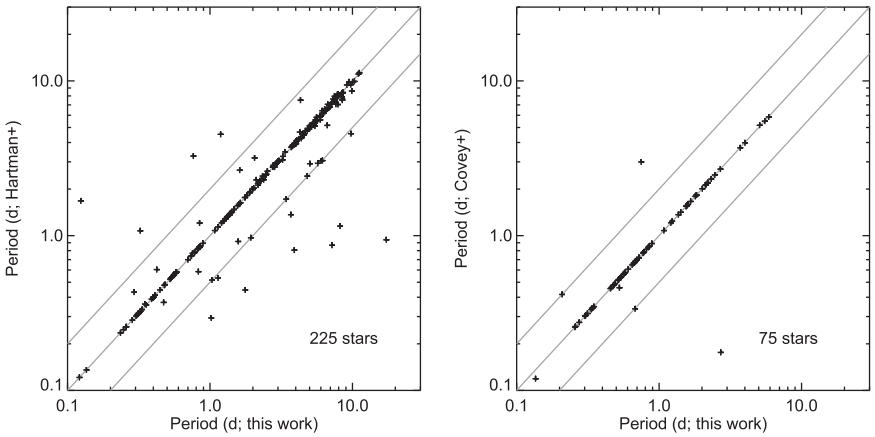

Figure 4. Left: objects with periods in both Hartman et al. (2010) and this work, compared. There are 225 objects in this plot, 85% of which agree to 10% or better. Right: objects with periods in both Covey et al. (2016) and this work, compared, with those from Hartman et al. removed. There are 75 objects in this plot, 92% of which agree to 10% or better. In both cases, there are three gray lines: a 1:1 match, and the $2P$ and $P/2$ harmonics. We conclude that that our approach to finding periods is working at least as well as those in the literature.

periodic. Those stars are listed Appendix B for reference, and those periods have been removed from subsequent analysis.

We find periods for 798 out of our sample of 1020 *K*2 LCs of candidate Pleiads. However, not all of those stars may be members; see Section 2.5.

2.3. Comparison to Literature Values

2.3.1. Literature Periods

In order to verify our period-finding approach, it is useful to compare to prior Pleiades results. There are two recent papers that obtain periods in the Pleiades from large-field photometric monitoring. Hartman et al. (2010) used HATNet and reported periods for 383 Pleiads. We have 225 periodic objects in common (given spatial and brightness constraints), and we agree to within 10% of the derived P for 85% of the objects; see Figure 4. The median fractional difference $(|(P_{\rm Hartman} - P_{\rm Rebull})|/P_{\rm Rebull})$ is 0.7%. Covey et al. (2016) used PTF and report periods for 138 Pleiads. We have 75 periodic objects in common with this study (again, given spatial and brightness constraints), and 92% of them agree to within 10% of the derived P; see Figure 4. The median fractional difference is 0.07%.

For each of the targets in which we have periods that disagree (or in which the literature reports a period that we did not find), we inspected our LC and associated power spectrum in some detail. There are several bright targets for which we failed to find a period where others did; in the *K*2 data, the star is just too bright for the data reduction used here. For most of the stars where our period is very discrepant from the published one, we believe that our period is correct for the stars at the time that we observed them. These discrepancies may be telling

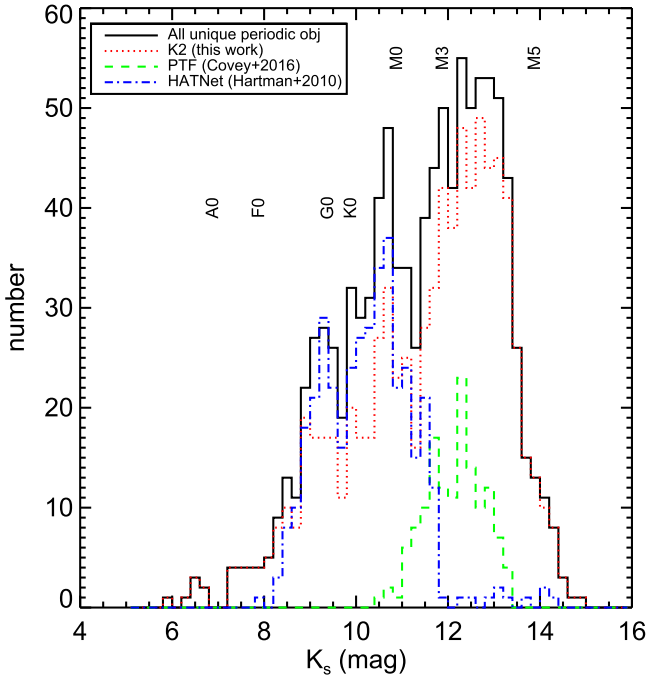

Figure 5. Comparison of range of K_s magnitudes for the entire set of periodic candidate Pleiads (black solid line), with subsamples indicated from *K*2 (this work), PTF (Covey et al. 2016), and HATNet (Hartman et al. 2010) as shown. Approximate spectral types corresponding to K_s in the Pleiades are annotated. There are 1184 unique objects shown here, the vast majority of which are Pleiades members (some are not necessarily members). The *K*2 study tremendously expands the number of known periodic objects, especially for fainter Pleiades stars. Objects that appear in more than one study are counted only once in the black histogram, but may appear once per study in the colored histograms. The Hartman and Covey studies include regions of the cluster not covered by *K*2.

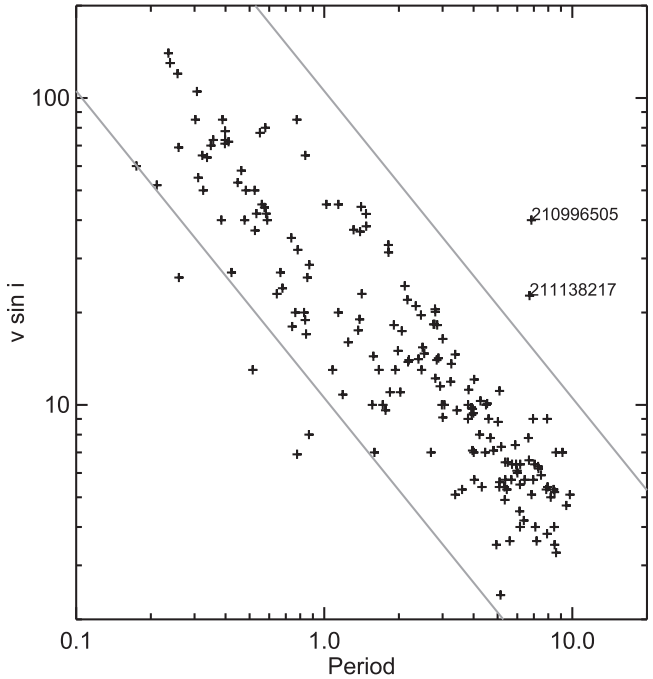

Figure 6. P (in days) vs. $v \sin i$ (in km s^{-1}) for stars in this study for which there are $v \sin i$ values in the literature. The gray lines correspond to the expected relationship between P and $v \sin i$ ($=(2\pi R \sin i)/P$) for $i = 90°$ and 6°, assuming $R = 0.5\ R_\odot$. The P and $v \sin i$ agree well, except for two cases—both of which are earlier-type stars with a secondary component, where the $v \sin i$ is probably from the primary and the P is from the lower-mass secondary. They are EPIC 210996505/HII1132 and 211138217/HII1766.

us something about the long-term spot distribution and/or spot evolution, but the details of that are beyond the scope of the present paper. EPIC 211089068/HII1348 has a period in Hartman et al. that is not quite a harmonic; they report 4.562 days, and we have 9.773 days. In three cases, the power spectrum and phased LC derived from our data alone are not as convincing as other sources in this study (e.g., the FAP is not 0 for these periodogram peaks), but since they independently recover the same period as reported in Covey et al., we have opted to keep them. They are 210978953/HHJ114, 211055493/JRS26, and 211083672/HCG253.

We conclude that our approach to finding periods is working at least as well as those in the literature.

Figure 5 demonstrates the range of K_s magnitudes to which the various studies are sensitive. The Hartman et al. (2010) study focused on the brighter stars, and the Covey et al. (2016) study focused on the fainter stars. This work, with *K*2, increases the number of periods known overall, but makes a more significant contribution of new periods for the fainter (lower-mass) stars. Note that this plot includes periods for 798 out of our 1020 *K*2 LCs; the literature reports periods for ~500 (candidate) Pleiads, so we have more than doubled the number of known periods for candidate Pleiads. (However, not all of the *K*2 LCs are for likely member stars; see Section 2.5.)

In the subsequent analysis here, we made a decision to not include periods from these literature studies for objects that did not have a *K*2 LC, which omits ~220 periods (not all of which may be members). Since the *K*2 target selection is primarily biased in position (Figure 1), and since rotation period is not a function of the location in the cluster, this does not affect our conclusions.

2.3.2. Literature v sin i

Much early work on rotation in the Pleiades was done on projected rotational velocities, $v \sin i$. Figure 6 shows the relationship between P and $v \sin i$ for stars in this study for which there are $v \sin i$ values in the literature (see Section 2.4). The P and $v \sin i$ agree well overall, which is an indication that we are measuring the rotation rate for these stars. The P and $v \sin i$ do not agree well for two cases, EPIC 210996505/HII1132 and 211138217/HII1766. These are both earlier-type stars that likely have a secondary component, where the $v \sin i$ is probably from the primary and the P is from the lower-mass secondary (see Paper III).

Both Jackson & Jeffries (2010) and Hartman et al. (2010) have already looked at the distribution of $\sin i$ in the Pleiades in detail. This kind of analysis is limited by the number of $v \sin i$ values known; although we are adding many periods here, there are no new $v \sin i$ values.

2.4. Supporting Data from the Literature

We assembled a catalog of photometric data for all of our targets from the literature, including Johnson & Mitchell (1958), Stauffer et al. (1998a, 1998b, 2007), Kamai et al. (2014), and Bouy et al. (2015). We added to this data from the Two Micron All Sky Survey (2MASS; Skrutskie et al. 2006); from the *Spitzer Space Telescope* (Werner et al. 2004), including measurements from Sierchio et al. (2010) and the

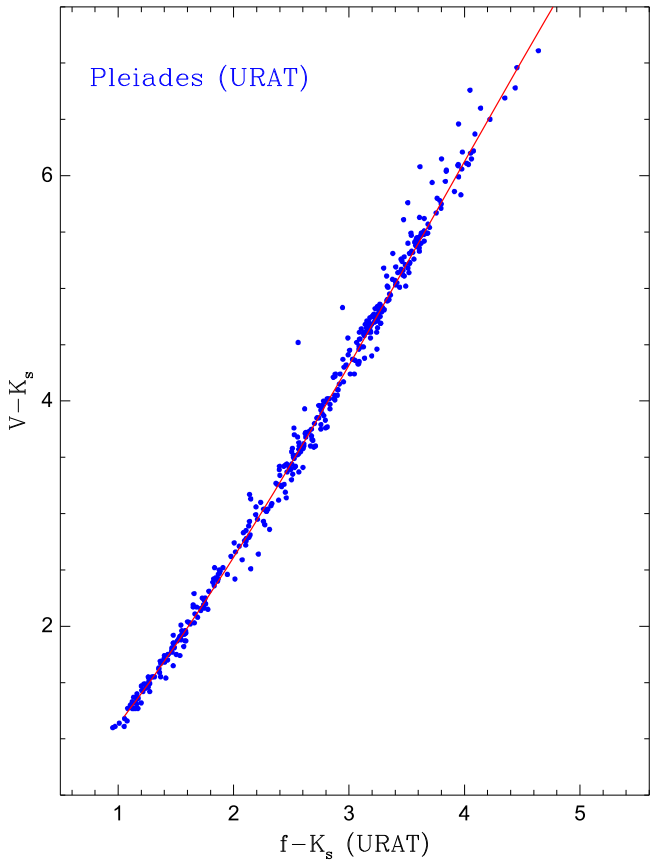

Figure 7. Empirical relationship between $V - K_s$ and $f - K_s$ (where the f comes from URAT). The best-fit line (Equation (3)) is the magenta line. We used this relationship to obtain estimates of $(V - K_s)_0$ for those stars for which we had no V measure; see text.

Spitzer Enhanced Imaging Products, SEIP[21]; from the *Wide-field Infrared Survey Explorer* (*WISE*; Wright et al. 2010); from SIMBAD's listing of the Tycho catalog (ESA 1997); and from the United States Naval Observatory (USNO) Robotic Astrometric Telescope (URAT; Zacharias et al. 2015).

Ideally, we would have $T_{\rm eff}$ or mass for all of our targets. However, those quantities can be very model dependent. Because we preferred to keep our discussion of the new *K*2 rotation period data on an empirical basis to the extent possible, our goal was to use an observed color as the proxy for mass or $T_{\rm eff}$. The broadband color that acts as the best such proxy over the entire mass range for which we have periods is $(V - K_{\rm s})_0$. While $K_{\rm s}$ is widely available from 2MASS, V is harder to find. We only have measured V-band photometry for about half of the periodic stars; it was necessary to estimate V magnitudes from other photometry for the rest.

The highest-quality V-band photometry we have is from phototube photometry reported in Johnson & Mitchell (1958), Landolt (1979), Stauffer & Hartmann (1987), or references therein, or CCD photometry from Kamai et al. (2014). Additional V-band photometry, generally for fainter members, was obtained using CCD cameras on small telescopes by Prosser et al. (1991) and Stauffer et al. (1998a). For the remaining stars (mostly faint M dwarfs), we have adopted measured photometry at bands near in wavelength to V. Specifically, we have adopted g or r magnitudes from SDSS-filter images reported in Bouy et al. (2013) or Bouy et al. (2015), or "f" magnitudes (a very broadband red filter) provided with the initial release of the URAT catalog (Zacharias et al. 2015) for all Pleiades members for which those quantitities are reported. For the stars for which we also have measured V magnitudes, we have then derived transformations between $r - K_s$, $r - K_s$, $f - K_s$, and $V - K_s$; Figure 7 shows the data for one such transformation. For each of these three data sources, the photometry appears to have similar accuracies to the available V-band photometry, and the transformations are well defined and not strongly curved. The three polynomial relations are

$$V - K_s = 0.3837 + 0.48719 \times (g - K_s) + 0.08564 \times (g - K_s)^2 - 0.00488 \times (g - K_s)^3 \quad \text{for} \quad 1.75 < g - K_s < 7.75 \tag{1}$$

$$V - K_s = -0.2991 + 1.47462 \times (r - K_s) - 0.07522 \times (r - K_s)^2 + 0.00394 \times (r - K_s)^3 \quad \text{for} \quad 1.0 < r - K_s < 6.25 \tag{2}$$

$$V - K_s = -0.004 + 0.91784 \times (f - K_s) + 0.23683 \times (f - K_s)^2 - 0.02080 \times (f - K_s)^3 \quad \text{for} \quad 1.0 < f - K_s < 4.75. \tag{3}$$

For most stars, we have these estimated $V - K_s$ values from all three sources. When we have a measured $V - K_s$, we use that; when we do not have a measured $V - K_s$, we use the average estimated $V - K_s$. Note that this is $K_{\rm s}$, not K_p, that is, K-short from 2MASS, not *Kepler* magnitude; $K_{\rm s}$ is used throughout this paper, and not K_p.

We assume that the typical reddening in the direction of the Pleiades applies: $A_v = 0.12$, $A_K = 0.01$, $E(B - V) = 0.04$ (Crawford & Perry 1976). There are four stars with *K*2 LCs that have larger reddening (HII476, HII870, HII1039, and HII1136); for these, we used reddening corrections from Soderblom et al. (1993b) and Breger (1986). Below, in the tables and figures, the observed V and $K_{\rm s}$ are tabulated separately and used where available; in those cases where we use an inferred $V - K_s$, that value is tabulated.

2.5. Membership and Definition of Sample

In order to establish the best possible set of Pleiades members, we evaluated each object using a combination of proper motions and photometric position in an optical color–magnitude diagram (CMD). We primarily used membership probabilities based on recent proper-motion studies (Bouy et al. 2015; see also Sarro et al. 2014 and Lodieu et al. 2012).[22] For objects where the membership probability and the photometric position were inconsistent, we evaluated stars on a case-by-case basis, comparing information from many sources, such as positions and proper motions, radial velocities, X-ray flux, IR flux, and Hα equivalent width. These values are from the literature, including Trumpler (1921), Hertzsprung (1947), Johnson & Mitchell (1958), Ahmed et al. (1965), Iriarte (1967), Artyukhina & Kalinina (1970), Jones (1970, 1973), Breger (1972, 1986), Morel & Magnenat (1978), Landolt (1979), Vasilevskis et al. (1979), Stauffer et al. (1984), van Leeuwen

[21] http://irsa.ipac.caltech.edu/data/SPITZER/Enhanced/SEIP/overview.html

[22] All objects analyzed by Lodieu et al. appear in Bouy et al. Some Lodieu et al. members are reassigned in Bouy et al., which has better proper motions and photometry. See discussion in Sarro et al. (2014).

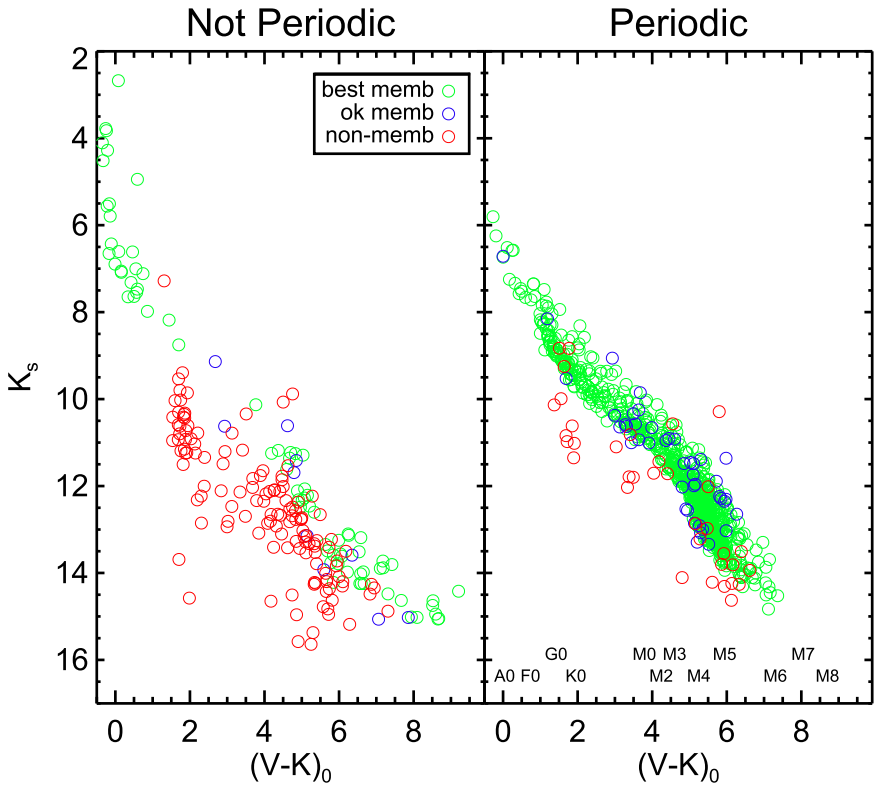

Figure 8. Optical CMD (K_s vs. $(V-K_s)_0$) for stars with $K2$ LCs and for which we could calculate $(V-K_s)_0$. Left panel is stars not measured to be periodic, and right panel is stars for which we could measure periods. Spectral types for a given $(V-K_s)_0$ are as shown in the bottom of the right panel. Green symbols are our best, highest-confidence sample of members, blue symbols correspond to those lower-confidence members (ok members), and red symbols are non-members. Most of the members have periods, and most are comfortably in the expected location of the main sequence. The non-members have considerably more scatter and fewer periods.

et al. (1986, 1987), Stauffer & Hartmann (1987), Jameson & Skillen (1989), Mermilliod et al. (1997, 2009), Micela et al. (1990, 1999), Prosser et al. (1991), Stauffer et al. (1991), Rosvick et al. (1992), Soderblom et al. (1993a), Kazarovets (1993), Hodgkin et al. (1995), Schilbach et al. (1995), Martin et al. (1996), Wang et al. (1996), Burkhart & Coupry (1997), Zapatero Osorio et al. (1997), Belikov et al. (1998), Stauffer et al. (1998a, 1998b), Queloz et al. (1998), Malaroda et al. (2000), Pinfield et al. (2000, 2003), Ducati (2002), Deacon & Hambly (2004), Li (2004), Scholz & Eislöffel (2004), Mermilliod (2006), Fox Machado et al. (2006, 2011), Gebran & Monier (2008), Renson & Manfroid (2009), Roeser et al. (2010; PPMXL), Lodieu et al. (2012), Zacharias et al. (2013; UCAC4), Cottaar et al. (2014), and Zacharias et al. (2014; URAT).

Our membership analysis usually began with the location of the star in a V versus $V-K$ CMD; in many cases, we also looked at other CMDs in order to make sure that a bad measurement in one band was not causing a discrepant CMD location. Next, usually we looked at proper-motion measurements in multiple studies (including the all-sky surveys like PPMX, UCAC4, URAT, etc.), again in order to attempt to minimize the influence of single "bad" measurement. If those steps did not yield an unambiguous decision, we next looked at all references to the star in SIMBAD in order to, for example, determine if any previous study had determined radial velocities or lithium equivalent widths or other data from which membership could be inferred (such as X-ray data). In a very few cases, we obtained new spectra to help determine membership (see Paper III). This process was qualitative in the sense that we weighted all of the information in a subjective manner. However, the process was also extensive, with each star considered individually and with all available information considered in detail. Based on the location of these stars in the CMD (Figure 8) and the fact that most of the non-members show no period in their $K2$ data (also Figure 8), we believe that in the great majority of cases we have made the right decision.

As a result of this analysis, we have a set of our highest-confidence members, for which there is considerable data supporting membership (often abbreviated as "best members"), and a set of non-members (NM). There is also a set of lower-confidence members (often abbreviated as "ok members"), where the evidence for membership is suggestive but not conclusive (e.g., all the proper-motion studies said it was an unambiguous member, but it was slightly too high or too low in one of the optical CMDs, and had insufficient data to place it in the other optical CMDs). Our final list of members (best or ok) is in Table 2 (for the periodic members) and Table 3 for the rest, and is what we carry forward here. The list of objects we investigated with $K2$ LCs but that we believe are not Pleiades members appears in Appendix D, along with derived periods where relevant. Figure 8 shows the optical CMD, K_s versus $(V-K_s)_0$, for stars with $K2$ LCs and for which we could obtain or calculate K_s and $(V-K_s)_0$. Many of the objects we took to be NM are clearly in a position inconsistent with membership.

Figure 8 also shows our effective bright and faint cutoffs. For $K_s \lesssim 6$ and $K_s \gtrsim 14.5$ (or $M_K \lesssim 0.5$ and $M_K \gtrsim 9$), the $K2$ LCs are either too bright or too faint to yield reliable periods using our approach. These objects are dropped from our sample going forward, and they appear as a list in the Appendix C.

Table 2
Contents of Table: Periods and Supporting Data for Periodic Pleiades Members

Label	Contents
EPIC	Number in the Ecliptic Plane Input Catalog (EPIC) for *K*2
Name	Position-based ID
RA	R.A. in decimal degrees (J2000)
Dec	Decl. in decimal degrees (J2000)
Vmag	*V* magnitude (in Vega mags), if observed
Kmag	K_s magnitude (in Vega mags), if observed
vmk0	$(V - K_s)_0$—dereddened $V - K_s$, directly observed (if *V* and K_s exist) or inferred (see text)
P1	Primary period, in days (taken to be rotation period)
P2	Secondary period, in days
P3	Tertiary period, in days
P4	Quaternary period, in days
ampl	Amplitude, in magnitudes, of the 10th to the 90th percentile
LC	LC used as "best"[a]
memb	Membership indicator: Best, OK, or NM
Plit	Literature (rotation) period, in days, if available
vsini	Literature $v \sin i$, in km s^{-1}, if available

Note.
[a] LC1—PDC, from MAST; LC2—version following A. M. Cody et al. (2016, in preparation); LC3—version following Aigrain et al. (2015, 2016); LC4—version reduced by Vanderburg & Johnson (2014) and downloaded from MAST.

(This table is available in its entirety in machine-readable form.)

Our set of members consists of 799 high-confidence ("best") Pleiades members and 54 more lower-confidence ("ok") members, for a total of 853. Thus, we find that 167 of the candidate Pleiads with *K*2 LCs are unlikely to be members (see Appendix D). Omitting the too bright and too faint stars for our sample, there are 775 high-confidence members, with 51 more lower-confidence members (for a total of 826 members). Out of those 775 (best members), 716 (92.4%) have at least one measured period that we believe in the overwhelming majority of cases to be a rotation period and due to starspots. Including the lower-confidence members, 759/826 (91.9%) have at least one measured period that we believe to be the rotation period. Table 1 summarizes the most important of these numbers. Table 2 includes all of these members and their measured periods. This sample of members (both "best" and "ok") that are within $6 < K_s < 14.5$ is hereafter the set of "members of the right brightness range," and is what our analysis is based on (unless otherwise specified). An online-only figure set with one set of plots (like those in Figure 2) for each star can be found in Appendix F.

We also scoured the literature for any information about binarity. This information came from Abt et al. (1965), Anderson et al. (1966), Stauffer et al. (1984), Liu et al. (1991), Mermilliod et al. (1992), Rosvick et al. (1992), Soderblom et al. (1993b), Bouvier et al. (1997), Queloz et al. (1998), Raboud & Mermilliod (1998), Geissler et al. (2012), and Kamai et al. (2014). We note here that most of these literature surveys focused on the brighter sources, and there are *K*2 data for many fainter stars. We discuss more about binaries below, primarily in Section 3.2, and in Papers II and III. (Note that Paper III also includes a description of how we identified photometric binaries.)

2.6. Members Not Detected as Periodic

As can be seen in Figure 8, about 8% of the sample are not detected as periodic in our data (see Appendix A for example LCs and power spectra). For these stars, one or more of these criteria are met: (a) no periodogram peaks with very low FAP in the LS output; (b) periodogram peak(s) change position significantly between LC versions, or the purported periodic signal appears as a peak in the periodograms in only one LC version; (c) phased LC does not look convincing (e.g., a wide distribution of fluxes at most phases) because the pattern is not well repeated from cycle to cycle; (d) LC obviously and signficantly affected by instrumental effects (e.g., bimodal distribution of flux values originating from saturated pixels); (e) rarely, the repeated pattern is not consistent with spot modulation. A list of those in the last category appear in Appendix B.

Some of these not-detected-as-periodic members can be found at nearly every color. The *K*2 data are exquisite, and we expect all stars to rotate, and low-mass stars as young as the Pleiades should have large starspots. There are several possible explanations as to why we do not detect these stars to be periodic. These stars could have periods much longer than 35 days, which is very unlikely for the Pleiades. Despite our best efforts, these stars could actually be non-members (and thus could have a period much longer than 35 days; with only 72 days of data, it would be hard to reliably identify a period much longer than 35 days). It could be that these stars have periodic variations on timescales <35 days but at a lower level than we can detect, perhaps from smaller spots/spot groups. The stars could have a rotation axis that is pole-on, such that there really is little to no variation detectable from our solar system. Alternatively, they could have disorganized spots distributed more or less homogeneously that preclude a reliably periodic signal in the LC. In about half of the cases, however,

Table 3
Supporting Data for Pleiades Members Not Detected to Be Periodic in the *K*2 Data[a]

EPIC	R.A., Decl. (J2000)	Other Name	*V* (mag)	K_s (mag)	$(V - K_s)_0$[b] (mag)	Membership
210784603	033103.57+193805.1	s3289407	…	10.13	3.77	best
210899735	033202.35+212310.8	…	…	12.11	4.89	best
210904850	033211.53+212756.1	UGCSJ033211.55+212755.7	…	13.90	7.11	best
210971138	033310.49+223119.3	DH027	15.55	11.25	4.19	best
211029507	033518.74+232621.0	DH045	…	13.98	6.22	best

Notes.
[a] Three stars from this table have periods in the literature : EPIC 211060530 (0.622 days), 211078009 (3.158 days), and 211094556 (0.17 days). We do not recover these periods from the *K*2 data.
[b] Dereddened $V - K_s$, directly observed (if *V* and K_s exist) or inferred (see text).

(This table is available in its entirety in machine-readable form.)

these LCs are corrupted by instrumental effects in the data reductions we have; either the stars are too bright themselves for reliable LCs, or nearby bright stars adversely affect the extracted LCs.[23] There are also several LCs that are just effectively too faint (poor signal-to-noise ratio [S/N]) for viable periods to be extracted from the data reductions we have. A period might have been detected for many of these not-detected-as-periodic member stars if the saturation level was higher, or the exposures different (longer for the poor S/N, shorter for the saturated), or if the star was located elsewhere on the CCD. Since we already detect periods in a very large fraction of the members, were it not for these non-astrophysical effects, the fraction could be even closer to 1. This is different than prior studies of rotation in clusters, and it means that we have an unusually complete view of the rotation distribution in the Pleiades.

Basic parameters for these stars not detected as periodic are listed in Table 3. Five of these stars have reported periods in the literature that we do not recover; see Table 3.

3. PERIOD AND PERIOD–COLOR DISTRIBUTIONS

As discussed above, the overwhelming majority of the periods we have determined are spot-modulated rotation periods of the stars. We can now proceed to investigate the distribution of rotation rates. In this section, we investigate the rotation distribution against $(V - K_s)_0$ color. Note that that we have selected only one P (and $(V - K_s)_0$) to be representative of the rotation period (and color) in the ~22% of the stars for which there is more than one period recovered (see Paper II).

3.1. Morphology of P versus $(V - K_s)_0$

Figure 9 shows the relationship between P and $(V - K_s)_0$ for the sample. It follows the overall trends found in other Pleiades studies (e.g., Hartman et al. 2010; Covey et al. 2016). There is a slowly rotating sequence for $1.1 \lesssim (V - K_s)_0 \lesssim 3.7$ (2 days $\lesssim P \lesssim$ 11 days) and a primarily rapidly rotating population for $(V - K_s)_0 \gtrsim 5.0$ (0.1 days $\lesssim P \lesssim$ 2 days). There is a region in which there seems to be a disorganized relationship between P and $(V - K_s)_0$ between $3.7 \lesssim (V - K_s)_0 \lesssim 5.0$ (0.2 days $\lesssim P \lesssim$ 15 days).

Another important thing to note is that the lower-confidence members still follow the overall trends here; there is no compelling evidence from this plot per se to move those lower-confidence members into the non-member set. (In contrast, see Appendix D and Figure 16 below.)

Among the long-period outliers in this plot, there are five stars with periods longer than 12 days, one of which is a lower-confidence member, but four of which are high-confidence members. Those long-P outliers are curious, since they seem out of place relative to the other members. These stars are discussed further in Paper III, though we highlight one here. We have taken EPIC 210855272/DH668 to have a period of 17.6 days for the reasons discussed in Paper II; that seems to be the best period. However, if we take $P = 8.9$ days (the other peak that appears in the periodogram), then this star would no longer be a long-period outlier; for its $(V - K_s)_0$, it would have a P more consistent with other stars of its color. It has Hα in absorption, but this may be acceptable for $(V - K_s)_0 = 3.6$ mag. At that color, it has the largest Hα absorption equivalent width in the Pleiades, comparable to a field star at that color. It has a 60% chance of being a member according to Deacon & Hambly (2004) and a 72% chance of being a member in Bouy et al. (2015); based on that, we have it as a lower-confidence member.

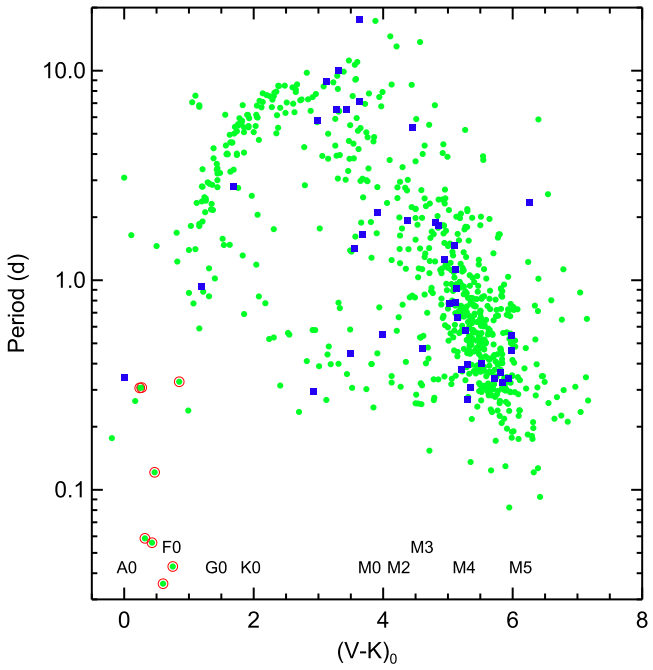

Figure 9. Plot of P vs. $(V - K_s)_0$ for the best members (green dots) and the lower-confidence members (blue squares). Pulsators (δ Scutis from Paper II) have an additional red circle. The distribution follows the same overall trends found in other Pleiades studies. There is a slowly rotating main sequence for $1.1 \lesssim (V - K_s)_0 \lesssim 3.7$ and a primarily rapidly rotating population for $(V - K_s)_0 \gtrsim 5.0$.

Among the blue short-period outliers, the stars we identify as pulsators in Paper II have demonstrably shorter periods on average (and are among the bluest stars) than the rest of the ensemble, and this matches expectations. There are other very blue stars that are not quite among the shortest periods. Their LC morphologies are more suggestive of rotation than pulsation. The stars with $P \sim 0.3$ days could also be pulsators (see Paper II). Normal A and F stars should not have spots, though Am stars could have spots (e.g., Balona et al. 2015). They could also be unresolved binaries, where the $(V - K_s)_0$ corresponds to the primary, but the P corresponds to the fainter, lower-mass, spotted secondary.

3.2. Binaries

Whether a star is single or is one component of a binary could affect the measured rotation period we detect in the $K2$ Pleiades data. This might be true because the formation mechanism for single and binary stars might have different dependencies either on the initial angular momentum of the collapsing cloud core or on how much of that angular momentum is retained in the zero-age main-sequence descendents of that process. In addition, being a member of a binary will affect the photometric colors we measure and the S/N properties of any periodic signature that we measure in the $K2$ data. We therefore have searched for the possible influence of binarity on the period distribution that we have

[23] Other investigators have methodologies to extract photometry and derive periods for very bright (saturated) stars (e.g., White et al. 2015), but these are not included here, in part because we do not have access to those data reductions, but also because we are primarily interested in the FGKM stars.

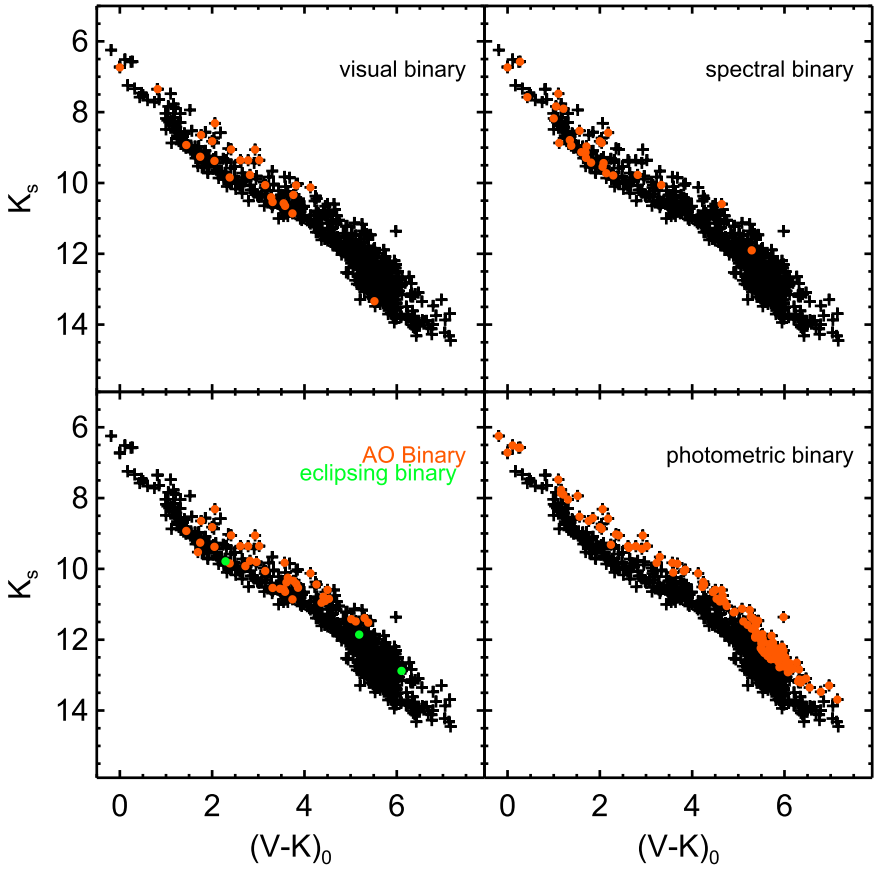

Figure 10. Plot of K_s vs. $(V - K_s)_0$, highlighting the binaries listed in the literature as found by a variety of literature methods (top left: visual binaries; top right: spectroscopic binaries; bottom left: AO (orange) and eclipsing binaries (green)), and in the lower right, the binaries just from position in the CMD as used here. The many approaches to identifying binaries identify different stars as binary.

measured. The discussion about the influence of binarity continues in Papers II and III.

We assembled binary information from the literature (see Section 2.5) from spectroscopy, radial velocities, high spatial resolution imaging, and new Robo-AO data (L. A. Hillenbrand et al. 2016, in preparation). The advantage of this inhomogenous data set is that we have a chance of identifying all of the binaries, but the disadvantage is that many existing surveys were limited spatially or limited by stellar brightness such that lack of binarity from this collection of data may actually reflect a lack of information rather than anything else. Figure 10 shows where these literature binaries fall in the CMD; Figure 11 shows P versus $(V - K_s)_0$ with the literature binaries highlighted. In these figures, visual binaries, spectroscopic binaries, binaries from AO observations, and eclipsing binaries are indicated separately. It is clear that most of the literature methods focused on bluer (brighter) stars. About 10% of the sample is tagged binary in the literature.

We can also use the optical CMD assembled here (Figure 8) to more uniformly identify photometric binaries by the stars' location in the CMD (see Paper III for details of this process). The advantage of this approach is that we can identify binaries with uniform sensitivity through the whole viable range of our data. The disadvantage is that we will miss binaries whose masses are significantly different from each other (i.e., causing only small shifts in the CMD). Figure 10 shows the CMD, and Figure 11 shows P versus $(V - K_s)_0$, for photometric binaries selected via this approach; about 16% of the sample is tagged binary.

The slow sequence has relatively few binaries identified, except for the spectroscopic binaries, and these are nearly all cases where no secondary has been directly detected. In these cases, the secondary is generally much fainter than the primary, and the secondary is therefore unlikely to be significantly affecting the $K2$ LCs. Even in the cases of the visual binaries in the slow sequence, many of the secondaries are much fainter than their primaries, and here too, the secondaries are unlikely to have much of an impact on the $K2$ LCs of these stars. Since the primary stars are in the "right place" in the P versus $(V - K_s)_0$ diagram for stars of their $(V - K_s)_0$ (mass), we infer that there is little influence on the primary's rotation rate by the much lower mass secondary for these binaries.

We continue the discussion about the influence of binarity in Papers II and III.

3.3. Amplitudes

We calculated the amplitude of the LCs in magnitudes by assembling the distribution of all points in the LC, taking the log of the 90th percentile flux, subtracting from that the log of the 10th percentile flux, and multiplying by 2.5. Figure 12 plots that amplitude against both P and $(V - K_s)_0$ for the periodic LCs. While the lower-amplitude variations are found at all periods, they tend to cluster at bluer colors; stars bluer than about $(V - K_s)_0 \sim 1.1$ (see Paper III) have distinctly lower amplitudes. Some of these stars are likely pulsators, which accounts for the lower amplitude. Some are probably unresolved binaries, where the amplitude of the flux variation

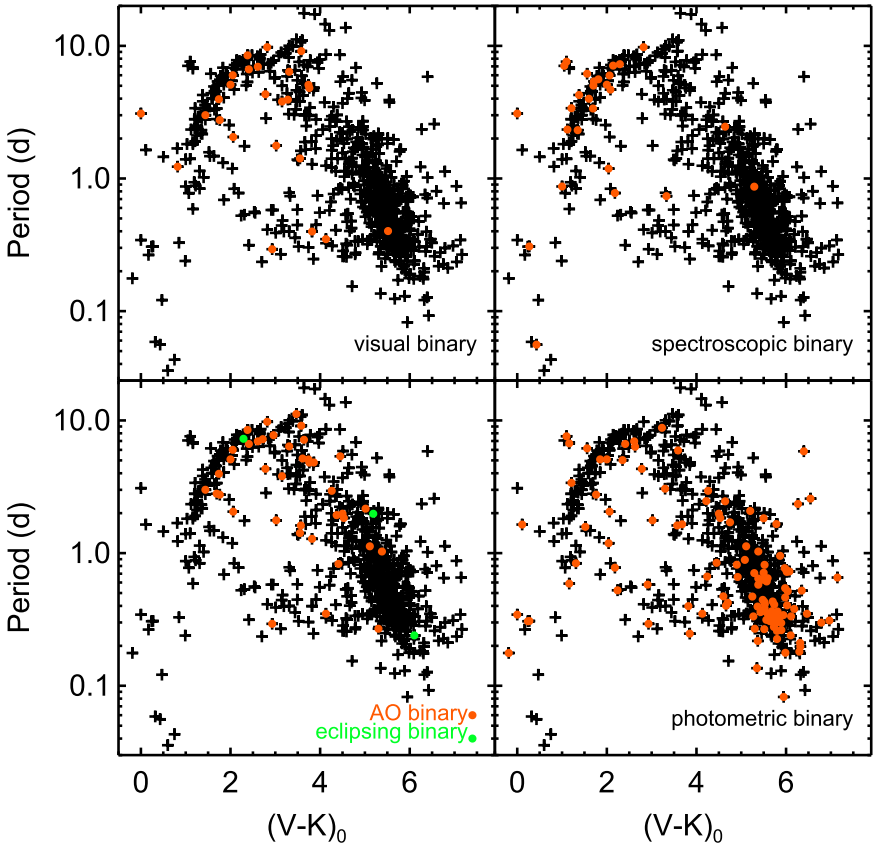

Figure 11. Plot of P vs. $(V - K_s)_0$, highlighting the binaries listed in the literature as found by a variety of literature methods (top left: visual binaries; top right: spectroscopic binaries; bottom left: AO (adaptive optics; orange) and eclipsing binaries (green)), and in the lower right, the binaries just from position in the CMD used here (Figure 8). While the many approaches to identifying binaries identify different stars as binary, there is no clear and obvious trend in the overall P vs. $(V - K_s)_0$ that simply segregates binaries from single stars; see text.

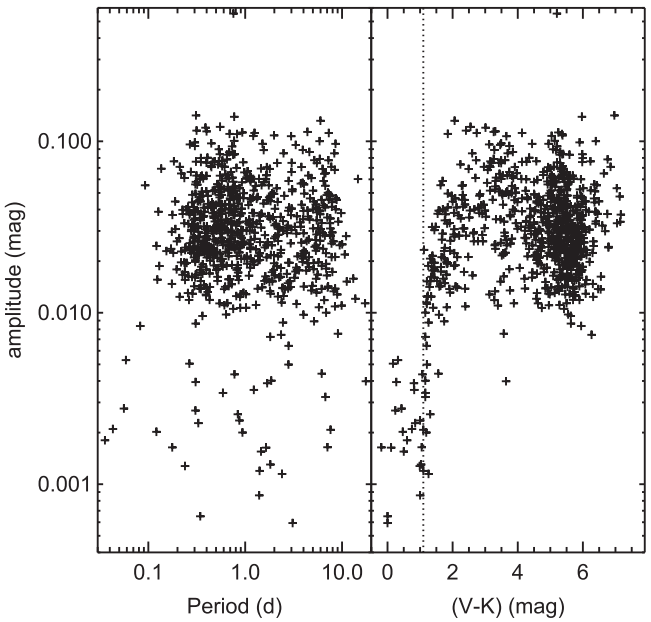

Figure 12. The amplitude (from the 10th to the 90th percentile), in magnitudes, of the periodic light curves, against P and $(V - K_s)_0$. The vertical dotted line is at $(V - K_s)_0 = 1.1$ (see Paper III, where there is a linear version of this plot). Stars bluer than about $(V - K_s)_0 \sim 1.1$ have clearly lower amplitudes. The median of the amplitude distribution (with or without the $(V - K_s)_0 < 1.1$ stars) is 0.030 mag.

from the companion (causing the periodicity) is lessened by the flux from the primary. The median of the amplitude distribution (with or without the $(V - K_s)_0 < 1.1$ stars) is 0.030 mag.

The outlier with the very large amplitude is 211010517/UGCSJ040234.77+230828.4, and it has a large amplitude because of a large-scale trend that is superimposed on the periodic LC. We have taken it to be one of the best (high-quality) members, but it is just barely in the expected location in the CMD to be placed in the best member subset.

Aside from the outliers at the small- and large-amplitude ends of the distribution, there does not seem to be a trend with color or period.

4. CONCLUSIONS

We have presented the first part of our analysis of the *K*2 Pleiades light curves, in the process vastly expanding the number of Pleiades members known with periods, particularly at the low-mass end. About 92% of the observed Pleiades members have at least one measured period, the overwhelming majority of which we believe to be spot-modulated rotation periods. For the ~8% of the members without periods, non-astrophysical effects often dominate (saturation, etc.), such that periodic signals might have been detectable, all other things being equal. We now have an unusually complete view of the rotation distribution in the Pleiades.

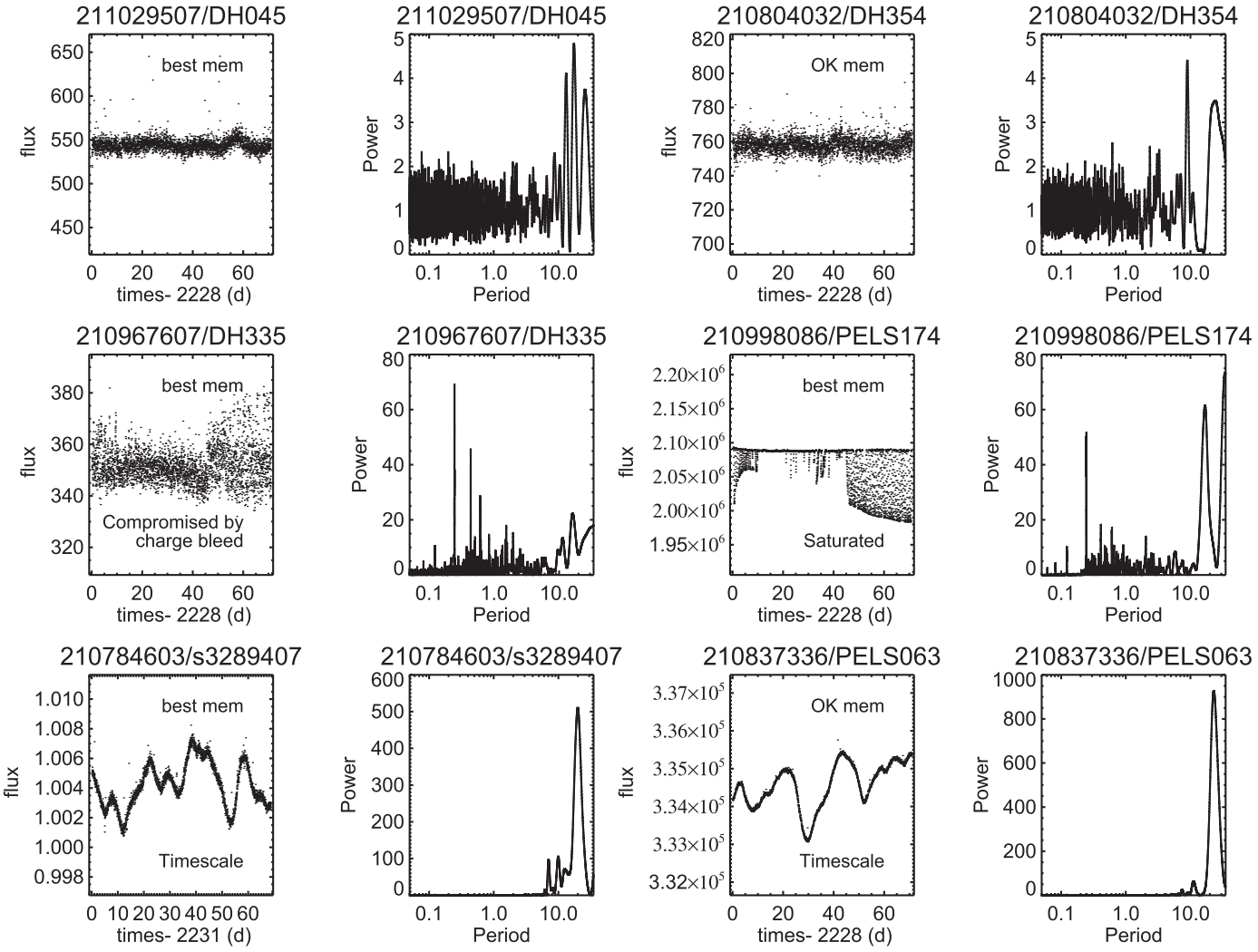

Figure 13. Full LC and power spectrum for six stars not detected as periodic by us. Stars, in order, L to R, top to bottom: 211029507/DH045 (best member; no significant periodogram peaks), 210804032/DH354 (OK member; no significant periodogram peaks), 210967607/DH335 (best member, but compromised by charge bleed), 210998086/PELS174 (best member, but saturated), 210784603/s3289407 (best member, but pattern irregular enough that this is a "timescale," not a rotation period; see Appendix B), 210837336/PELS063 (OK member, but pattern irregular enough that this is a "timescale," not a rotation period; see Appendix B).

The overall relationship between P and $(V-K_s)_0$ follows the overall trends found in other Pleiades studies. There is a slowly rotating sequence for $1.1 \lesssim (V-K_s)_0 \lesssim 3.7$ (2 days $\lesssim P \lesssim$ 11 days) and a primarily rapidly rotating population for $(V-K_s)_0 \gtrsim 5.0$ (0.1 days $\lesssim P \lesssim 2$ days). There is a region in which there seems to be a disorganized relationship between P and $(V-K_s)_0$ between $3.7 \lesssim (V-K_s)_0 \lesssim 5.0$ (0.2 days $\lesssim P \lesssim 15$ days).

Thanks in no small part to the many low-mass fast rotators, the distribution of periods peaks strongly at <1 day; only ~3% of the periods are longer than 10 days. The typical amplitude of the variation (between 10% and 90% of the distribution of points) is ~0.03 mag. Some much lower amplitudes can be found at the bluest colors, which could be from pulsation or a consequence of binarity (where the lower-mass, fainter star is responsible for the spot-modulated rotation period).

Our periods agree well with the literature periods and literature $v \sin i$. There is no simple way to distinguish binaries from single stars in the P versus $(V-K_s)_0$ parameter space.

About 70% of the periodic stars have a single, essentially stable period. However, we have discovered complicated multiperiod behavior in Pleiades stars using these *K*2 data, and we discuss this further in Paper II. Paper III (Stauffer et al. 2016) continues the discussion by speculating on the origin and evolution of the periods in the Pleiades.

We thank R. Stern and T. David for helpful comments on draft manuscripts. A.C.C. acknowledges support from STFC grant ST/M001296/1.

Some of the data presented in this paper were obtained from the Mikulski Archive for Space Telescopes (MAST). Support for MAST for non-*HST* data is provided by the NASA Office of Space Science via grant NNX09AF08G and by other grants and contracts. This paper includes data collected by the *Kepler* mission. Funding for the *Kepler* mission is provided by the NASA Science Mission directorate.

This research has made use of the NASA/IPAC Infrared Science Archive (IRSA), which is operated by the Jet Propulsion Laboratory, California Institute of Technology, under contract with the National Aeronautics and Space Administration. This research has made use of NASA's Astrophysics Data System (ADS) Abstract Service and of the SIMBAD database, operated at CDS, Strasbourg, France. This research has made use of data products from the Two Micron

Table 4
Timescales

EPIC	Name	R.A. (J2000) (deg)	Decl. (J2000) (deg)	Other Name	Timescale (days)	Membership	Notes
210784603	033103.57+193805.1	52.76490	19.63475	s3289407	20	best memb	…
210909681	033326.45+213229.8	53.36022	21.54162	s4679029	22	NM	…
211018285	033652.52+231545.2	54.21886	23.26258	DH065	16.81	ok memb	Possibly rotation period or possibly timescale
211071563	033935.45+240706.3	54.89773	24.11842	HHJ407	33	best memb	…
211063756	034218.86+235922.2	55.57860	23.98952	SK687	18	NM	…
211020453	034512.69+231746.5	56.30291	23.29626	HII580	~25	NM	…
211114664	034554.25+244806.7	56.47605	24.80189	WCZ114	~18	NM	…
210837725	034705.34+202639.5	56.77226	20.44432	s4798986	~30	ok memb	…
211045908	035122.47+234219.1	57.84365	23.70533	BPL234	~26	NM	…
211026586	035146.55+232334.7	57.94398	23.39299	BPL241	24	NM	…
210914077	035202.47+213637.7	58.01031	21.61049	DH735	~28	NM	…
211020039	035203.61+231721.5	58.01506	23.28931	SK202	29	NM	…
210837336	035208.80+202618.9	58.03669	20.43860	PELS063	23	ok memb	…
210928539	035225.91+215031.8	58.10799	21.84219	DH752	30	NM	…
211132831	035242.50+250702.9	58.17710	25.11750	SRS33701	~12.5	NM	…
211063255	035321.59+235854.2	58.33996	23.98173	SK132	~35	NM	…
211044588	035359.92+234100.3	58.49968	23.68343	BPL296	~5.2	NM	…
211082538	035507.08+241725.8	58.77952	24.29050	SK67	~25–30	NM	…
211051964	035549.89+234822.7	58.95788	23.80632	BPL332	~35	NM	…
211145558	035621.72+252110.4	59.09051	25.35291	BPL336	23	NM	"Bursts," not spots
211050613	035626.19+234703.5	59.10914	23.78433	DH835	15-30	NM	Hard to know which period is right
210751596	035721.70+190803.4	59.34042	19.13428	UGCSJ035721.71+190803.2	~25	NM	Only see repeated pattern in one LC version
211110418	035852.12+244348.5	59.71720	24.73015	UGCSJ035852.13+244348.3	~25	NM	…
211137552	040049.31+251210.9	60.20548	25.20305	DH895	~29	NM	…
211038138	040105.79+233444.3	60.27414	23.57897	UGCSJ040105.81+233443.8	~20	best memb	…
211005312	040154.08+230331.6	60.47535	23.05878	s4337464	19.579	NM	This could be a spot period
211026906	040437.17+232351.5	61.15490	23.39764	s5092529	~25	best memb	…
211045801	041001.97+234212.3	62.50823	23.70343	s4634206	long, ~50d?	NM	…

(This table is available in machine-readable form.)

Table 5
Targets That Are Too Bright or Too Faint

EPIC	Name	R.A. (J2000) (deg)	Decl. (J2000) (deg)	Other Name	Period(s) (days)	Membership
210967871	033228.28+222806.5	53.11785	22.46849	DH019	…	ok memb
211075945	034133.76+241118.6	55.39068	24.18852	BPL24	0.496079	NM
211068507	034248.16+240401.4	55.70070	24.06706	BPL45	…	best memb
211110493	034300.16+244352.5	55.75069	24.73126	BPL49	…	best memb
211096282	034340.29+243011.4	55.91790	24.50318	BPL62	…	best memb
211097372	034353.54+243111.6	55.97309	24.51991	BPL66	…	best memb
211082490	034448.21+241722.2	56.20089	24.28950	Caeleno = HII447	…	best memb
200007769	034452.53+240647.8	56.21888	24.11328	Electra = HII468	…	best memb
211116936	034509.73+245021.3	56.29058	24.83927	HII541	0.674473, 0.647851	best memb
200007772	034512.50+242802.1	56.30209	24.46726	Taygeta = HII563	…	best memb
200007771	034549.60+242203.7	56.45667	24.36770	Maia = HII785	…	best memb
210976082	034550.40+223606.0	56.46004	22.60167	BPL78	…	ok memb
211073549	034550.64+240903.7	56.46104	24.15104	BPL79	…	best memb
211099592	034554.47+243316.2	56.47697	24.55450	Asterope = HII817	…	best memb
200007770	034619.58+235654.1	56.58160	23.94838	Merope = HII980	…	best memb
211086019	034623.11+242036.3	56.59630	24.34342	BPL100	…	ok memb
211138940	034702.53+251345.6	56.76056	25.22934	BPL123	…	NM
211106625	034705.70+244003.7	56.77376	24.66771	BPL124	0.267422	best memb
211094511	034712.09+242832.0	56.80039	24.47558	BPL132	…	best memb
211088076	034717.91+242231.6	56.82466	24.37546	BPL137	…	NM
210983090	034723.97+224237.3	56.84989	22.71038	BPL142	0.304403, 0.247935	best memb
200007767	034729.08+240618.4	56.87118	24.10512	Alcyone = etaTau = HII1432	…	best memb
211102808	034739.00+243622.3	56.91254	24.60622	BPL152	…	best memb
211090981	034819.00+242512.9	57.07918	24.42027	BPL172	…	NM
211028385	034820.81+232516.5	57.08672	23.42127	HII1823	…	best memb
210993392	034825.60+225212.3	57.10669	22.87009	BPL179	…	NM
200007768	034909.74+240312.1	57.29060	24.05337	Atlas = HII2168	…	best memb
200007773	034911.21+240812.0	57.29672	24.13667	Pleione = HII2181	…	best memb
211048942	035125.55+234521.3	57.85648	23.75593	BRB14	…	best memb
211029838	035144.91+232639.5	57.93716	23.44431	BPL240	…	best memb
211123454	035157.11+245706.5	57.98796	24.95181	DH729	…	NM
210914077	035202.47+213637.7	58.01031	21.61049	DH735	…	NM
211131711	035323.34+250550.5	58.34725	25.09738	BPL284	…	NM
211069099	035334.54+240438.2	58.39392	24.07729	BPL287	…	NM
211135437	035415.27+250952.3	58.56365	25.16453	BPL306	…	best memb
211140205	035444.19+251511.1	58.68413	25.25310	BPL316	…	NM
211115616	035523.07+244905.2	58.84613	24.81813	BPL327	0.231512	best memb
211103918	035622.33+243723.4	59.09307	24.62319	DH832	…	NM
211080216	035634.19+241513.1	59.14250	24.25366	DH838	…	NM
210981512	035639.65+224112.2	59.16524	22.68674	DH842	…	NM
211085541	035758.48+242008.8	59.49368	24.33580	DH861	…	NM

(This table is available in machine-readable form.)

Table 6
Targets Taken as Non-members

EPIC	R.A., decl. (J2000)	Other Name	V (mag)	K_s (mag)	$(V - K_s)_0$	Period (days)
210979798	032928.08+223936.2	s5035799	…	11.10	3.03	29.564
210978791	033008.26+223838.9	DH010	…	12.77	4.98	…
211004869	033035.37+230308.3	DH012	…	14.26	5.33	…
210909681	033326.45+213229.8	s4679029	…	11.21	2.94	…
210960667	033338.99+222108.9	DH029	…	13.44	4.95	…
210931896	033617.62+215339.1	AKII293	11.00	9.25	1.64	4.370
210953848	033626.15+221445.7	DH057	…	12.53	4.68	…
210820939	033629.04+201119.8	UGCSJ033629.05+201119.6	…	12.47	3.12	…
210833806	033753.23+202301.7	UGCSJ033753.25+202301.2	…	12.75	4.98	…

(This table is available in its entirety in machine-readable form.)

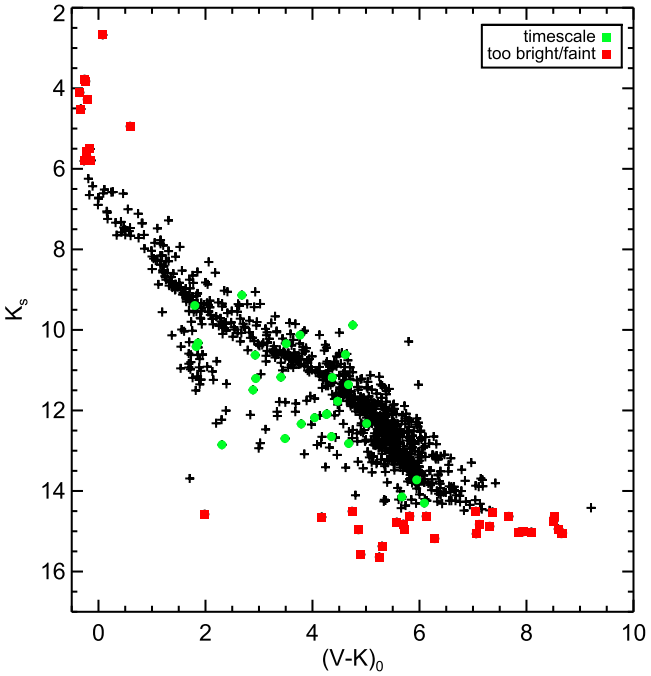

Figure 14. Optical CMD (K_s vs. $(V-K_s)_0$) for the ensemble (plus signs), those sources with timescales as opposed to spot periods (green circles), and those sources that are too bright or faint for us to obtain a complete sample of periods (red squares). Timescales only appear for $2 < (V-K_s)_0 < 8$. It is not clear whether these signatures come from spots or not.

All-Sky Survey (2MASS), which is a joint project of the University of Massachusetts and the Infrared Processing and Analysis Center, funded by the National Aeronautics and Space Administration and the National Science Foundation. The 2MASS data are served by the NASA/IPAC Infrared Science Archive, which is operated by the Jet Propulsion Laboratory, California Institute of Technology, under contract with the National Aeronautics and Space Administration. This publication makes use of data products from the *Wide-field Infrared Survey Explorer*, which is a joint project of the University of California, Los Angeles, and the Jet Propulsion Laboratory/California Institute of Technology, funded by the National Aeronautics and Space Administration.

Facilities: Kepler, *K2*, *Spitzer*, 2MASS.

APPENDIX A
EXAMPLES OF MEMBERS NOT DETECTED AS PERIODIC

Section 2.6 above mentions member stars not detected by us as periodic. Here are six examples of these kinds of stars. In the top row, 211029507/DH045 and 210804032/DH354 both have flat LCs with no significant periodogram peaks. In the second row, 210967607/DH335 and 210998086/PELS174 both have LCs compromised by saturated pixels, either from themselves or from a nearby bright star. In the last row, 210784603/s3289407 and 210837336/PELS063 both have somewhat of a repeated pattern, but this pattern is irregular enough that we have designated these as having a "timescale," not a rotation period; see Appendix B.

APPENDIX B
TIMESCALES

For some objects, we found a period during our analysis, but individual inspection of the LCs suggests that whatever is causing the repeating pattern is not a spot-modulated rotation period. For examples of such patterns, see Figure 13; for a complete list of these objects, see Table 4. We have opted to describe the period suggested by the repeating pattern as a "timescale" rather than a period. In several cases, they are also non-members. They do not really have a preferential color; see Figure 14. However, this figure also demonstrates that many of the timescale objects are photometric non-members. For comparison, Figure 13 includes two examples of timescale objects that are members.

The repeating pattern in EPIC 211005312/s4337464 is the most borderline case, by which we mean that this LC could conceivably be a spot-modulated signal; see Figure 15. However, it is a non-member.

In one case, EPIC 211145558 = BPL336, the LC texture resembles the "bursts" from NGC 2264, characterized by Stauffer et al. (2014) as accretion bursts (see Figure 15). This object is not a member of the Pleiades; it could be a member of Taurus, suggesting that an interpretation of accretion bursts is not impossible. It does not have a clear IR excess (it is detected only at the shortest two bands of *WISE*, and [3.4] $-$[4.6] = 0.3 mag). It is located very far to the east and somewhat to the north of the Pleiades cluster center, toward where Taurus members are. Another possibility, of course, is that all the structure is instrumental, not real, but this structure is found in all of the LC versions we have. It is listed as a photometric member in Pinfield et al. (2003), though the proper motions in URAT are not consistent with Pleiades membership, and Bouy et al. (2015) also have it as a clear NM.

For completeness, we note that the actual eclipses in the eclipsing binaries, which also have a repeating pattern that is not a rotation period, are not included here, but appear in David et al. (2015, 2016).

APPENDIX C
STARS THAT ARE TOO BRIGHT OR TOO FAINT FOR THIS SAMPLE

We empirically determined that our brightness and faintness limits are effectively $K_s \lesssim 6$ and $K_s \gtrsim 14.5$, respectively. Sometimes, despite these limits, we were still able to derive a period (and in two cases, two distinct periods). In Table 5, we list those objects that are too bright or too faint for our sample.

APPENDIX D
NON-MEMBERS

There are more than 150 stars where a *K*2 LC was obtained, presumably because SIMBAD or other literature considered these objects as Pleiades members. However, consideration of each of the individual stars, including the references mentioned above in Section 2.5, suggests that these are not, in fact, likely to be Pleiades members. They are listed in Table 6 with the period(s) we derived, and plotted (where possible) in Figure 16. Only about 20% of these objects have periods, which is a significantly lower rate than that for the members, consistent with these being a different population. Note also that several of the NM have repeated patterns that we believe to not be

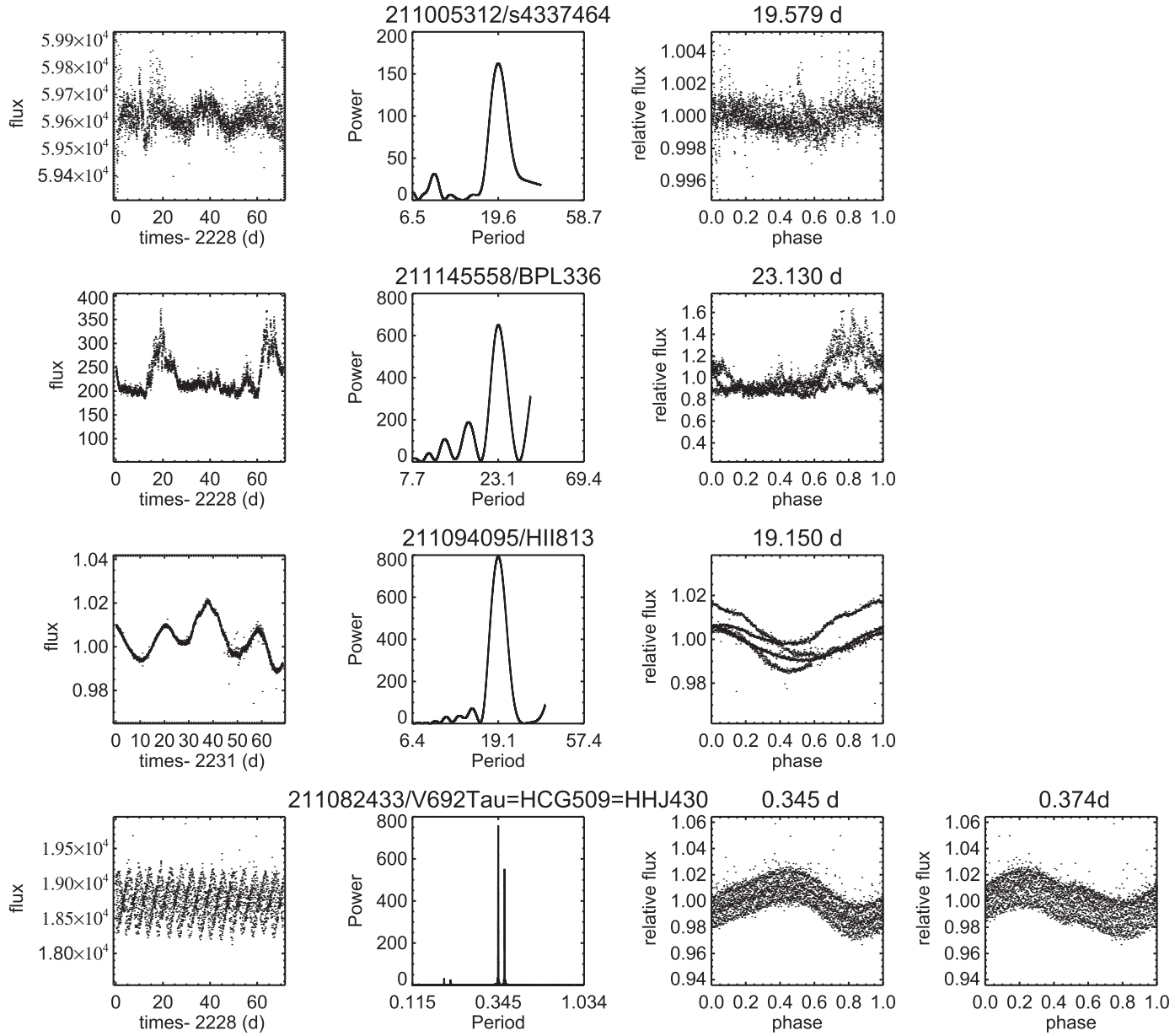

Figure 15. Full LC (first column), power spectrum (second column), and phased LC for primary period (third column) and secondary period (fourth column) for apparent non-members (rows, in order) 211005312/s4337464 (most likely of these to be a spot-modulated rotation period, but a non-member), 211145558/BPL336 (resembles the very young "bursters" found in NGC 2264), 211094095/HII813 (could plausibly be a spot period, but a non-member), and 211082433/V692Tau = HCG509 = HHJ430 (LC that looks like other members, but it is too high in the optical CMD to be a member).

spot-modulated, periodic signals; these timescales are listed in Appendix B. EPIC 211145558/BPL336 (in Figure 15) is discussed there.

EPIC 211094095/HII813 is one peculiar case worthy of additional discussion. It has a very long period for a Pleiades member (19.15 days; see Figure 15). The LC shape is plausibly due to spot modulation. It has an 84% chance of membership in Deacon & Hambly (2004), a 6% chance of membership in Belikov et al. (1998), a 48% chance of membership in Stauffer et al. (1991), but a 98% chance of membership in Bouy et al. (2015). Its motion in R.A. is very discrepant from the ensemble Pleiades motion, though the actual measurements in the literature cover a much wider range than for other members of comparable brightness. We have declared it an NM based on an unpublished HIRES spectrum (discussed in Paper III). Its radial velocity is about 5–8 km s^{-1} too high. If it is a member, its very long period would have to be explained in the context of models of rotational evolution.

EPIC 211082433/V692Tau = HCG509 = HHJ430 is another peculiar case. It has two significant periods like many of the other Pleiades members; see Figure 15. It appears too high in the optical CMD for us to consider it a member. It has a 2% chance of being a member in Belikov et al. (1998), 0% in Kazarovets (1993), 17% in Stauffer et al. (1991), and 16% in Bouy et al. (2015). On the other hand, it is one of two stars that Oppenheimer et al. (1997) report has a high Li abundance, which means that it is almost certainly young. We have opted to leave it as an NM, but it is quite puzzling nonetheless. Interestingly, there is a "glitch" in the

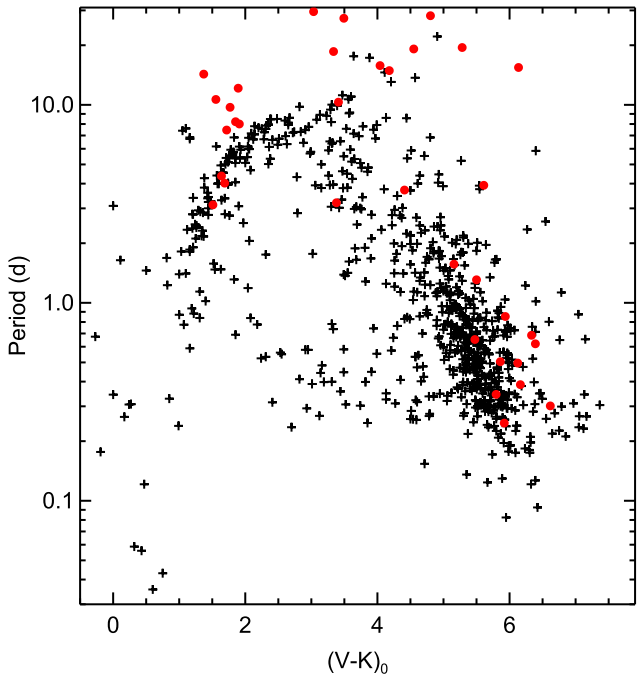

Figure 16. Plot of P vs. $(V - K_s)_0$ for the ensemble discussed in the rest of the paper (black plus signs) and the non-members for which we have a period (red circles). They are more often longer periods than the rest of the distribution at a given $(V - K_s)_0$, consistent with being a non-member.

Table 7
Contents of Online Cross-identifications List

Label	Contents
EPIC	Number in the Ecliptic Plane Input Catalog (EPIC) for *K*2
Name	More common name used here
HII	Name in HII catalog (Hertzsprung 1947)
HCG	Name in HCG catalog (Haro et al. 1982; Kazarovets 1993)
HHJ	Name in HHJ catalog (Hambly et al. 1993)
PELS	Name in Pels catalog (van Leeuwen et al. 1986)
DH	Name in DH catalog (Deacon & Hambly 2004)
SRS	Name in SRS catalog (Schilbach et al. 1995; Belikov et al. 1998)
BPL	Name in BPL catalog (Pinfield et al. 2000)
SK	Name in SK catalog (Stauffer et al. 1991)
Tr	Name in Tr catalog (Trumpler 1921)
WCZ	Name in WCZ catalog (Wang et al. 1996)
Simbad	Name used in Simbad as primary identifier
Lodieu	Name in Lodieu et al. (2012) catalog
Bouy	Name in Bouy et al. (2015) catalog
2MASS	Name in 2MASS All-sky point source catalog
tm6x	Flag for 2MASS 6x data

(This table is available in its entirety in machine-readable form.)

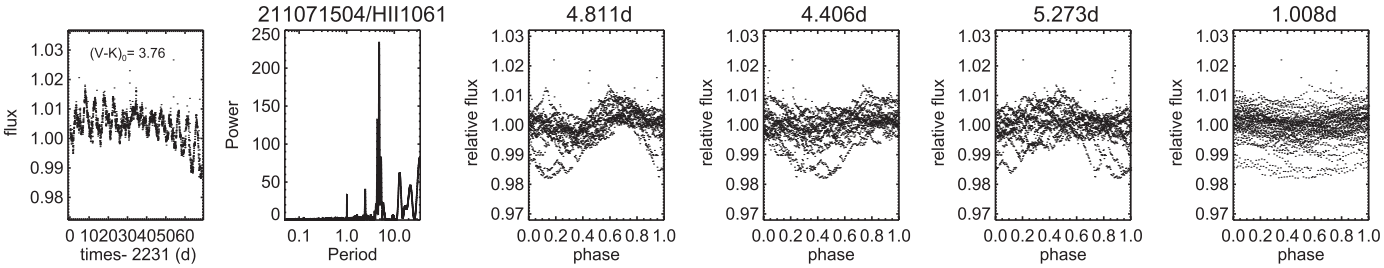

Figure 17. Example figure set figure: EPIC 211071504 (aka HII1061) with a primary period of 4.8107 days. Panels, from the left: original light curve (in units of flux), the power spectrum, and the phased light curve (in relative flux) for each viable period, for up to a total of four periods.

(The complete figure set (759 images) is available.)

phased LC at 0.374 days; the other of the two stars with Li is HCG332, discussed in Paper II as having angular dips. It could be that this "glitch" in HCG509 is a similar effect to that in HCG332. There is no compelling evidence for IR excess in HCG509.

APPENDIX E
CROSS-IDS

This section gives some of the common synonyms for our targets in the literature. The table is available in its entirety in the online version; a description of the columns appears in Table 7.

APPENDIX F
PHASED LCS: FIGURE SET

This section consists of an online-only figure set. Each periodic member (e.g., each source in Table 2) has a figure set element in Figure 17. Note that many of these sources have up to four periods that we identify; see Paper II for more discussion of these sources. The plots in each figure set file consist of the original LC (in units of flux), the power spectrum, and the phased LC (in relative flux) for each viable period, for up to a total of four periods.

REFERENCES

Abt, H., Barnes, R., Biggs, E., & Osmer, P. 1965, ApJ, 142, 1604
Ahmed, F., Lawrence, L., & Reddish, V. 1965, PROE, 3, 187
Aigrain, S., Hodgkin, S., Irwin, M., Lewis, J., & Roberts, S. 2015, MNRAS, 447, 2880
Aigrain, S., Parvianinen, H., & Pope, B. 2016, MNRAS, 459, 2408
Akeson, R., Chen, X., Ciardi, D., et al. 2013, PASP, 125, 989
Anderson, C., Stoeckly, R., & Kraft, R. 1966, ApJ, 143, 299
Artyukhina, N., & Kalinina, E. 1970, TrSht, 40, 3

Balona, L., Catanzaro, G., Abedigamba, O., Ripepi, V., & Smalley, B. 2015, MNRAS, 448, 1378
Balona, L., Guzik, J., Uytterhoeven, K., et al. 2011, MNRAS, 415, 3531
Balona, L., Krisciunas, K., & Cousins, A. 1994, MNRAS, 290, 905
Belikov, A., Hirte, S., Meuseinger, H., Piskunov, A., & Schilbach, E. 1998, A&A, 332, 575
Bouvier, J., Matt, S., Mohanty, S., et al. 2014, in Protostars and Planets VI, ed. H. Beuther et al. (Tucson, AZ: Univ. Arizona Press), 433
Bouvier, J., Rigaut, F., Nadeau, D., et al. 1997, A&A, 323, 139
Bouy, H., Bertin, E., Moraux, E., et al. 2013, A&A, 554, 101
Bouy, H., Bertin, E., Sarro, L., et al. 2015, A&A, 577, 148
Breger, M. 1972, ApJ, 176, 367
Breger, M. 1986, ApJ, 309, 311
Burkhart, C., & Coupry, M. 1997, A&A, 318, 870
Cottaar, M., Covey, K., Meter, M., et al. 2014, ApJ, 794, 125
Covey, K., Agüeros, M., Law, N., et al. 2016, ApJ, 822, 81
Crawford, D., & Perry, C. 1976, AJ, 81, 419
David, T., Conroy, K., Hillenbrand, L., et al. 2016, AJ, 151, 112
David, T., Stauffer, J., Hillenbrand, L., et al. 2015, ApJ, 814, 62
Deacon, N., & Hambly, N. 2004, A&A, 416, 125
Ducati, J. 2002, CDS/ADC Collection of Electronic Catalogues, 2237, 0
ESA 1997, The Hipparcos and Tycho Catalogues, ESA SP-1200, VizieR Online Data Catalog
Fox Machado, L., Michel, R., Álvarez, M., Fu, J., & Zurita, C. 2011, RMxAX, 40, 237
Fox Machado, L., Pérez Hernández, F., Suárez, J., Michel, E., & Lebreton, Y. 2006, A&A, 446, 611
Gebran, M., & Monier, R. 2008, A&A, 483, 567
Geissler, K., Metchev, S., Pham, A., et al. 2012, ApJ, 746, 44
Hambly, N., Hawkins, M., & Jameson, R. 1993, A&AS, 100, 607
Haro, G., Chavira, E., & Gonzalez, G. 1982, BITon, 3, 3
Hartman, J., Bakos, G., Kovács, G., & Noyes, R. 2010, MNRAS, 408, 475
Hertzsprung, E. 1947, AnLei, 19, 1
Hodgkin, S., Jameson, R., & Steele, I. 1995, MNRAS, 274, 869
Howell, S., Sobeck, C., Haas, M., et al. 2014, PASP, 126, 398
Iriarte, B. 1967, BOTT, 4, 79
Jackson, R., & Jeffries, R. 2010, MNRAS, 402, 1380
Jameson, R., & Skillen, I. 1989, MNRAS, 239, 247
Johnson, H., & Mitchell, R. 1958, ApJ, 128, 31
Jones, B. 1970, AJ, 75, 563
Jones, B. 1973, A&AS, 9, 313
Kamai, B., Vrba, F., Stauffer, J., & Stassun, K. 2014, AJ, 148, 30
Kazarovets, E. 1993, PZ, 23, 141
Kovács, G., Zucker, S., & Mazeh, T. 2002, A&A, 391, 369
Krisciunas, K. 1994, ComAp, 17, 213
Landolt, A. 1979, ApJ, 231, 468
Li, J.-Z. 2004, ChJAA, 4, 258
Liu, T., Janes, K., & Bania, T. 1991, ApJ, 377, 141
Lodieu, N., Deacon, N., & Hambly, N. 2012, MNRAS, 422, 1495
Malaroda, S., Levato, H., Morrell, N., et al. 2000, A&AS, 144, 1
Martin, E., Rebolo, R., & Zapatero-Osorio, M. 1996, ApJ, 469, 706
Melis, C., Reid, M., Mioduszewski, A., Stauffer, J., & Bower, G. 2014, Sci, 345, 1029
Mermilliod, J.-C. 2006, http://adsabs.harvard.edu/abs/2006yCat.2168....0M
Mermilliod, J.-C., Bratschi, P., & Mayor, M. 1997, A&A, 320, 74
Mermilliod, J.-C., Mayor, M., & Udry, S. 2009, A&A, 498, 949
Mermilliod, J.-C., Rosvick, J., Duquennoy, A., & Mayor, M. 1992, A&A, 265, 513
Micela, G., Sciortino, S., Harnden, F., et al. 1999, A&A, 341, 751
Micela, G., Sciortino, S., Vaiana, G., et al. 1990, ApJ, 348, 557
Morel, M., & Magnenat, P. 1978, A&AS, 34, 477
Oppenheimer, B., Basri, G., Nakajima, T., & Kulkarni, S. 1997, AJ, 113, 296
Pinfield, D., Dobbie, P., Jameson, R., et al. 2003, MNRAS, 342, 1241
Pinfield, D., Hodgkin, S., Jameson, R., et al. 2000, MNRAS, 313, 347
Plavchan, P., Jura, M., Kirkpatrick, J. D., Cutri, R. M., & Gallagher, S. C. 2008, ApJS, 175, 191
Prosser, C., Schild, R., Stauffer, J., & Jones, B. PASP, 105, 269
Prosser, C, Shetrone, M., Dasgupta, A., et al. 1995, PASP, 107, 211
Prosser, C, Shetrone, M., Marilli, E., et al. 1993, PASP, 105, 1407
Prosser, C, Stauffer, J., & Kraft, R. 1991, AJ, 101, 1361
Queloz, D., Allain, S., Mermilliod, J.-C., Bouvier, J., & Mayor, M. 1998, A&A, 335, 183
Raboud, D., & Mermilliod, J.-C. 1998, A&A, 329, 101
Rebull, L., Stauffer, J., & Cody, A. 2016, AJ, 152, 114 (Paper II)
Renson, P., & Manfroid, J. 2009, A&A, 498, 961
Roberts, D., Lehar, J., & Dreher, J. 1987, AJ, 93, 968
Roeser, S., Demleitner, M., & Schilbach, E. 2010, AJ, 139, 2440
Rosvick, J., Mermilliod, J.-C., & Mayor, M. 1992, A&A, 255, 130
Sarro, L., Bouy, H., Berihuete, A., et al. 2014, A&A, 563, 45
Scargle, J. D. 1982, ApJ, 263, 835
Schilbach, E., Robichon, N., Souchay, J., & Guibert, J. 1995, A&A, 299, 696
Scholz, A., & Eislöffel, J. 2004, A&A, 421, 259
Sierchio, J., Rieke, G., Su, K., et al. 2010, ApJ, 712, 1421
Skrutskie, M., Cutri, R. M., Stiening, R., et al. 2006, AJ, 131, 1163
Soderblom, D., Jones, B., Balachandran, S., et al. 1993a, AJ, 106, 1059
Soderblom, D., Stauffer, J., Hudon, J. D., & Jones, B. 1993b, ApJS, 85, 315
Stauffer, J. 1984, ApJ, 280, 189
Stauffer, J., Cody, A., Baglin, A., et al. 2014, AJ, 147, 83
Stauffer, J., Hartman, L., Soderblom, D., & Burnham, N. 1984, ApJ, 280, 202
Stauffer, J., & Hartmann, L. 1987, ApJ, 318, 337
Stauffer, J., Hartmann, L., Fazio, G., et al. 2007, ApJS, 172, 663
Stauffer, J., Klemola, A., Prosser, C., & Probst, R. 1991, AJ, 101, 980
Stauffer, J., Rebull, L., Bouvier, J., et al. 2016, AJ, 152, 115 (Paper III)
Stauffer, J., Schild, R., Baliunas, S., & Africano, J. 1987, PASP, 99, 471
Stauffer, J., Schild, R., Barrado y Navascués, D., et al. 1998a, ApJ, 504, 805
Stauffer, J., Schultz, G., & Kirkpatrick, J. D. 1998b, ApJ, 499, 199
Terndrup, D., Stauffer, J., Pinsonneault, M., et al. 2000, AJ, 119, 1303
Trumpler, R. 1921, LicOB, 10, 110
van Leeuwen, F., Alphenaar, P., & Brand, J. 1986, A&AS, 65, 309
van Leeuwen, F., Alphenaar, P., & Meys, J. 1987, A&AS, 67, 483
Vanderburg, A., & Johnson, J. 2014, PASP, 126, 948
Vasilevskis, S., van Leeuwen, F., Nicholson, W., & Murray, C. 1979, A&AS, 37, 333
Wang, J., Li, C., Zhao, J., & Jiang, P. 1996, AcASn, 37, 68
Werner, M., Roellig, T., Low, F., et al. 2004, ApJS, 154, 1
White, T., Aerts, C., Antoci, V., et al. 2015, in K2 Conf. http://lcogt.net/files/K2SciCon/Tim_White-White_Pleiades_K2SciCon.pdf
Wright, E., Eisenhardt, P. R. M., Mainzer, A. K., et al. 2010, AJ, 140, 1868
Zacharias, N., Finch, C. T., Girard, T. M., et al. 2013, AJ, 145, 44
Zacharias, N., Finch, C., Subasavage, J., et al. 2015, AJ, 150, 101
Zapatero Osorio, M., Rebolo, R., & Martin, E. 1997, A&A, 317, 164